

Fire spread between industry premises

Anders Lönnermark and Haukur Ingason
Brandforsk project 602-071

SP Technical Research Institute of Sweden



Abstract

Fire spread between industry premises

This report presents results and analysis from model scale tests carried out to validate calculation methods for estimation of the risk for fire spread between buildings. The basic parameters necessary to determine the risk for fire spread are: flame height and the incident thermal radiation. Knowledge about both these parameters is vital in order to estimate the risks properly. There is a lack of experimental information that considers the following important aspects influencing the propensity of a fire to jump from one industrial premise to another: heat release rate, size of an opening in a flashed over building, flame height and incident thermal radiation at different distances from the burning building. This report provides new data and better understanding of necessary input for such calculations. The model scale tests show good correspondence between a simple method to calculate heat radiation from a point source and experimental data obtained. Further, a simple and robust method to measure incident heat radiation is examined and evaluated.

Key words: industrial fires, fire spread, radiation, model scale tests

SP Sveriges Tekniska Forskningsinstitut
SP Technical Research Institute of Sweden

SP Report 2010:18
ISBN 978-91-86319-56-4
ISSN 0284-5172
Borås 2010

Contents

	Abstract	3
	Contents	4
	Preface	5
	Sammanfattning	6
	Nomenclature	10
1	Introduction	11
2	Theoretical aspects	13
2.1	Scale modelling	13
2.2	Scaling laws	13
2.3	Calculation of incident heat radiation	14
2.4	Flame height	15
2.5	Heat flux measurements	16
3	Experimental set-up	18
3.1	Scale-model of industrial premises	18
3.2	Measurements	19
3.3	Fuel	21
4	Experimental procedure	23
5	Results	24
5.1	Heat release rate	24
5.2	Temperature	29
5.3	Flame heights	30
5.4	Heat flux	32
5.4.1	Comparison of heat flux measurements	32
5.4.2	Comparison between plate thermometers and heat flux meters	36
6	Discussion	38
7	Conclusion	40
8	References	41
Appendix 1	Test protocols	44
Appendix 2	Time-resolved graphs	51

Preface

This project has been financed by the Swedish Fire Research Board (BRANDFORSK). In connection to the project start, an advisory group was created. This advisory group consists of the following people from a variety of different fire disciplines:

Erik Almgren	Bengt Dahlgren AB
Staffan Bengtson	Brandskyddslaget
Mikael Asplund	Trygg-Hansa
Patrick Van Hees	Lunds Tekniska Högskola LTH
Samuel Nyström	Räddningstjänsten i Jönköping
Daniel Gillesén	Räddningstjänsten StorGöteborg
Jennie Werner	Räddningstjänsten StorGöteborg
Lars Hellsten	Scania CV AB
Erik Nilsson	SSAB Tunnbrått AB
Sören Lundström	Myndigheten för samhällsskydd och beredskap (MSB)
Magnus Nordberg	Brandkonsulten AB
Jörgen Carlsson	ÅF Infrastruktur AB
Jonas Roosberg	IKEA Risk Management Group
Staffan Abrahamsson	Boverket
Joel Jacobsson	Södra Älvsborgs Räddningstjänstförbund
Thomas Mohlén	Sandvik Materials Technology

We would like to thank the advisory group for their contribution to this work, especially Samuel Nyström at the Jönköping Rescue Service, who initiated the work. We appreciate the interest and guidance from Samuel and other members of the advisory group.

The technicians Michael Magnusson, Lars Gustafsson, Tarmo Karjalinen and Sven-Gunnar Gustafsson at SP Fire Technology are acknowledged for their valuable assistance during performance of the tests. They were also responsible for the construction of the test rig. Håkan Modin is acknowledged for his help with analysing video recordings.

Sammanfattning

Varje år inträffar ett antal stora bränder i industrilokaler. Egendomsskadorna kan bli mycket omfattande, speciellt om branden utvecklas snabbt och brandbelastningen är hög. Risken för brandspridning till närbelagda byggnader blir påtaglig speciellt om räddningstjänsten inte alltid har möjlighet att bekämpa branden om byggnaden inte är sprinklad. I icke sprinklade lokaler är kravet att byggnaden ska placeras och anordnas så att branden inte sprids till närliggande byggnader.

Allmänna rådet i dagens byggnadsregler [1] när det gäller skydd mot brandspridning mellan byggnader (5:72) är att den infallande strålningsnivån bör understiga 15 kW/m^2 under minst 30 minuter. Det innebär att nödvändiga beräkningar normalt genomförs när byggnaden är helt övertänd och lågor slår ut genom fönster eller tak. Detta allmänna råd blir först och främst aktuellt när man bestämmer sig för att inte sprinkla en byggnad. I dag arbetar man med funktionsbaserade regelsystem vilket innebär att man kan beräkna den kritiska strålningsnivån mot en närbelagd industribyggnad. Problemet idag är att det inte finns några bra verktyg för beräkning av fullt utvecklade bränder i industrilokaler. Beräkning av till exempel flammhöjd, som i sin tur används för strålningsberäkning mot närbelagda industribyggnader, bygger till stor del på modeller som är framtagna för öppna poolbränder och inte fullt utvecklade bränder. En viktig parameter att bedöma är brandens effektutveckling och geometriska förutsättningar. En avgörande fråga är hur höga flammorna är, hur dessa flammhöjder är i jämförelser med befintliga ingenjörsmoeller samt vilka parametrar i det aktuella scenariot som styr flammhöjden. Normalt är flammhöjden för dessa stora bränder lägre än vad som ges av de vanliga flammhöjdsmodellerna.

Även byggnadskonstruktionens brandtekniska utformning kan få en avgörande betydelse för resultaten. Beräkningsresultaten kan variera beroende på hur och när flammorna bryter igenom takkonstruktionen. Det kan vara många mindre flammor som slår ut genom fönsteröppningar eller en hög flamma som uppstår när hela eller delar av taket rasar in. Inverkan av yttre vind har också en stor betydelse på resultatet. Det finns ett stort behov av att undersöka och utvärdera de verktyg som används i dag för att beräkna brandspridningsrisken mellan byggnader. Vilka begränsningar finns det, vilka parametrar är det som styr och vilka parametrar bör man ta hänsyn till för att kunna göra relevanta beräkningar? För att utröna detta har en serie modellförsök genomförts som kan ge indikation på tillförlitligheten i de beräkningsmodeller som finns.

I rapporten redovisas genomförande och resultat från ett antal modellskaieförsök som genomfördes i skala 1:10. Huvudsyftet med brandförsöken var att studera flammhöjd och strålning, och att utvärdera de beräkningsmodeller som används för att uppskatta risken för brandspridning. Tyvärr fanns ingen möjlighet att utvärdera modellerna där hänsyn till vind tas. Modellen hade dimensionerna $6 \text{ m} \times 3 \text{ m} \times 0,7 \text{ m}$ och simulerade en industrilokal i fullskala med måtten $60 \text{ m} \times 30 \text{ m} \times 7 \text{ m}$. Som brandkälla användes stora träribbstaplar, vilka tändes med hjälp av heptan. Dessa brandkällor valdes för att få en så jämn brand som möjligt under en relativt lång tidsperiod samtidigt som vi ville att branden skulle täcka en tillräckligt stor golvyta för att motsvara en utbredd brand i en industrilokal. Totalt genomfördes tio försök där framför allt antalet öppningar och öppningsarean varierades för att simulera portar och hål i tak respektive vägg.

Resultaten visar att öppningarnas storlek och placering på ett signifikant sätt påverkar strålningen och därmed risken för brandspridning. Genom att samla upp brandgaserna i en stor huv kunde brandeffekten (den viktigaste parametern) mätas. Tillsammans med uppmätt flammhöjd och strålning kan olika beräkningsmodeller för infallande strålning mot närliggande byggnader valideras. Något som var väldigt tydligt under försöksserien var

att inte bara öppningarna i taket påverkar. Öppningar i väggarna, som simulerar öppna portar (tilluft), har signifikant inverkan på brandeffekten. En enkelport motsvarar i fullskala en port $4\text{ m} \times 4\text{ m}$, medan en dubbelport i fullskala är $8\text{ m} \times 4\text{ m}$ (i det aktuella fallet användes en sådan dubbelport på vardera gaveln, med en total area motsvarande 64 m^2 i fullskala). Hålet i taket varierades under försöksserien och motsvarar 5 %, 15 % eller 25 % av takarean. Man ser tydligt inverkan som avståndet har på den infallande strålningen, vilket följer de vanliga trenderna att strålning avtar med avståndet.

Vidare visade försöken att öppningarna på sidorna av modellbyggnaden och i taket har en avgörande betydelse för hur branden utvecklas. Små öppningar i taket påverkar branden, eftersom ventilationen blir sämre inne i lokalen. Storleken på öppningarna på väggarna har också stor betydelse på brandens utveckling, men dock inte i samma grad som taköppningen. Försöken visar att flamhöjden påverkas av brandens storlek och öppningens area. De högsta flamhöjderna uppnåddes när takarean var 15 % av den totala takytan, samt när tilluftsöppningarna på gaveln var som störst. Den infallande strålningsnivån på den längst utplacerade strålningsmätaren, det vill säga 3 m, låg på en nivå som var $2\text{--}5\text{ kW/m}^2$ och på den mätare som var närmast, det vill säga 0.5 m, uppmättes högst 46 kW/m^2 . Motsvarande värden i fullskala, förutsatt att modellen är i skala 1:10, är $6\text{--}15\text{ kW/m}^2$ upp till 145 kW/m^2 på avstånd som är 30 m respektive 5 m.

En jämförelse mellan beräknad flamhöjd och observerad flamhöjd från försöken gjordes. Den visar att de traditionella sambanden för öppna poolbränder behöver modifieras, mest när det gäller diameterberoendet av brandkällan. I övrigt överensstämde flamhöjdsekvationen bra med de som finns i litteraturen. Det enkla antagandet att betrakta flamman som punktkälla fungerade bra när man antog $\frac{1}{4}$ av flamhöjden som centrum punkt. När $\frac{1}{2}$ flamhöjden användes som punktkälla var överensstämmelsen dålig. Synfaktormetoden fungerade betydligt sämre jämfört med den korrigerade punktkällametoden, speciellt ju närmare observationpunkten var placerad.

Ingen undersökning gjordes på inverkan av yttre vind på resultaten.

Executive summary

Every year there are a number of large fires on industrial premises. Property damage can be extensive, especially if the fire develops rapidly and the fire load is high. Emergency services are not always able to fight the fire if the building is not sprinklered. In buildings where there are no sprinklers, the basic idea is that the building should be located and arranged so that the fire can not spread to nearby buildings.

The National Board of Housing, Building and Planning (Boverket) describe in the current building regulations that the protection against fire spread between buildings can only be guaranteed if the incident radiation level is less than 15 kW/m^2 for at least 30 minutes [1]. This means that the necessary calculations should normally be carried out when the building has reached complete flashover and the flames have burst through the windows or ceilings. This general aspect is, first and foremost, an issue when considering non-sprinklered buildings. Due to the new performance based regulatory system, calculations can be applied instead of using the table values. This requires that those conducting the calculations report credible estimate solutions. The problem today is that there are no validated tools for the calculation of a fully developed fire in an industrial building. For example, the calculation of flame height, which is used for the radiation calculation, is based largely on models that are designed for open pool fires and not fully developed fires in large industrial premises. An important parameter to assess is the effect of fire development and geometric conditions on these calculation methods. Normally the flame height from a large industrial fire is smaller than what is given by the most common flame height models.

Construction fire design can have a decisive influence on the results. Calculation results may vary depending on how and when the flames break through the ceiling. There may be many smaller flames, which burst through the window openings or a high flame, which occurs when all or part of the ceiling is collapsing. Therefore, there is a great need to examine and evaluate the tools used today to calculate the fire spread risk between the buildings.

A number of model-scale tests were conducted at a scale of 1:10. The main objective of the fire experiments was to study flame height and heat flux, and to evaluate the model used to estimate the risk of fire spread. The model had the dimensions of $6 \text{ m} \times 3 \text{ m} \times 0.7 \text{ m}$ and simulated industrial premises in full scale measuring $60 \text{ m} \times 30 \text{ m} \times 7 \text{ m}$. The fire source used was large wood cribs, which was lit with the help of heptane. These fire sources were used to get as uniform a fire as possible for a relatively long period of time. The fire was expected to cover a large enough floor space to meet the widespread fires in industrial premises. A total of ten tests were performed. The number of openings and the opening area was varied to simulate ports of the building and holes in ceiling and walls. By collecting the combustion gases in a hood connected to the exhaust system, the HRR was measured (the most important design parameter). Together with the measured flame height and heat flux, different modelling techniques for incident radiation to neighbouring structures were validated.

The openings in the walls simulated open ports, and the results show that they have a significant influence on fire development. A simple port equivalent in full scale to $4 \text{ m} \times 4 \text{ m}$, and a double gate corresponding to $8 \text{ m} \times 4 \text{ m}$ (in this case a double port on each gable was used with a total area representing 64 m^2 in full scale). The size of the hole in the ceiling was varied during the test series corresponding to 5 %, 15 % or 25 % of the total ceiling area. The test results show that the opening size and placement in a significant way affect the radiation and the risk of fire spread. Compared to free burning conditions, the maximum HRR is increased by 14 % with 5 % opening in the ceiling and

increased by 40 % for the case when the ceiling opening covered 15 % of the ceiling. It is interesting to note is that if the opening gets larger, some of the re-radiation effects are reduced and the HRR is also reduced. With the openings in the ceiling, the HRR become larger than when the opening is along the wall and it becomes larger if the opening is located centrally in the building than closer to the wall. This can be explained by the possibility of the fresh air coming in through the inlet openings to access to the combustion area. When the openings are centred in the ceiling the fresh air entrain more symmetric compared when the air can only access from one side. Further, when there are only small openings in the ceiling the fire becomes ventilation controlled. The highest HRR was only about one third of the free burn HRR.

The largest flame heights were obtained when the ceiling opening corresponded to 15 % of the total ceiling area, and the openings at the gables corresponded to the large double ports. The heat flux to the radiation meter that were positioned furthest away from the building was at a level that was 2-5 kW/m² and at the heat flux meter that were located closest, i.e. 0.5 m, up to 46 kW/m². The corresponding values in full scale, provided that the model is in 1:10 scale, is in the range of 6 to 15 kW/m² and up to 145 kW/m² at a distance which is 30 m and 5 m, respectively. This means that the validation of the models are covered within the range that is of interest in large scale i.e. 15 kW/m² and a distance that is up to 30 m.

A comparison was made using the point source model for calculation heat fluxes at different distance from the flame. The traditional way of using the equation, i.e. assuming $\frac{1}{2}$ the flame height in order to calculate the distance between the fire source and the receiver (heat flux meter), did not work very well. By changing the position representing the radiation point source, it was found that the best agreement between measured and calculated heat fluxes was obtained when $\frac{1}{4}$ of the flame height was chosen instead. A comparison was also made using the view factor method (solid flame model). The results were found to be very poor close to the wall (fire), and become increasingly better as the distance increased.

There are some aspects that still need to be addressed, but have not been included in this study. One such issue is the effects of external wind on the flame height geometry.

Nomenclature

c	Heat capacity (kJ/kg/K)
D	Diameter (m)
E	Released energy per consumed mass oxygen (kJ/kgO ₂)
Fr	Froude number
h	Convective heat transfer coefficient (kW/m ² /K)
h_f	Flame height (m)
Δh_c	Heat of combustion (kJ/kg)
K_{cond}	Conduction correction factor (kW/m ² /K)
L	Length (m)
m	Mass (kg)
\dot{q}	Incident heat flux by radiation (kW/m ²)
Q	Energy (kJ)
\dot{Q}	Heat release rate (kW)
t	Time (s)
T	Temperature (K)
u	Velocity (m/s)
\dot{V}	Volume flow (m ³ /s)

Greek

δ	Thickness (m)
ε	Surface emissivity (-)
ρ	Density (kg/m ³)
σ	Stefan-Boltzmann constant (kW/m ² /K ⁴)

Subscripts

comb	Combustion
F	Full scale
M	Model scale
rad,in	Incident radiation

Abbreviations

HFM	Heat flux meter
HRR	Heat release rate
O1 – O3	Opening 1 – Opening 3
PT	Plate thermometer
SB	Schmidt-Boelter
TC	Thermocouple
V1 – V4	Ventilation opening 1 – 4 in the ceiling

1 Introduction

Every year there are a number of large fires on industrial premises. Property damage can be extensive, especially if the fire develops rapidly and the fire load is high. Emergency services are not always able to fight the fire if the building is not sprinklered. In buildings where there are no sprinklers, the basic idea is that the building should be located and arranged so that the fire can not spread to nearby buildings. The National Board of Housing, Building and Planning (Boverket) describe in the current building regulations that the protection against fire spread between buildings can only be guaranteed if the incident radiation level is less than 15 kW/m^2 for at least 30 minutes [1]. This means that the necessary calculations should normally be carried out when the building has reached complete flashover and the flames have burst through the windows or ceilings. This general aspect is, first and foremost, an issue when considering non-sprinklered buildings.

Previously, and to some extent still today, designers used table values indicating the maximum net area for different levels of protection and the fire load in industrial buildings. The safety measures that were required, such as ventilators, was based on net room area (m^2) and the fire load (MJ/m^2) in the room. Due to the new performance based regulatory system, calculations can be applied instead of using the table values. This requires that those conducting the calculations report credible estimate solutions. The problem today is that there are no validated tools for the calculation of a fully developed fire in an industrial building. For example, the calculation of flame height, which is used for the radiation calculation, is based largely on models that are designed for open pool fires and not fully developed fires in large industrial premises. An important parameter to assess is the effect of fire development and geometric conditions on these calculation methods.

In the case of fire development rate there are no specific instructions about what curves to use for the calculation of fire growth in industrial premises. Fire engineers usually choose between the ultra-fast, fast, medium or slow curves [2]. The choice will vary from case to case. A non-sprinklered warehouse can today, for example, be designed for an ultra-fast curve with a maximum of either 15 MW and 40 MW, depending on the consultant doing the work. After the fire has reached a maximum value, the heat release rate is assumed to be constant until the calculation period ends. In reality the fire development does not always stop at 15 MW or 40 MW. Actually, it is more likely that a fire in an industrial building will be significantly higher than that. The link between fire growth and if and when the building / fire the cell reaches flashover is, therefore, important to understand.

Construction fire design can have a decisive influence on the results. Calculation results may vary depending on how and when the flames break through the ceiling. There may be many smaller flames, which burst through the window openings or a high flame, which occurs when all or part of the ceiling is collapsing. Therefore, there is a great need to examine and evaluate the tools used today to calculate the fire spread risk between the buildings.

The work presented here focuses on flames coming out of holes in the ceiling and how this affects the incident radiation towards a neighbouring building. A flashover situation is created inside the model, and the flames that burst out are documented. The heat radiation from the fire is then measured and compared to different calculation models available. A literature study, that contains several different calculations methods and large industrial fires, has been carried out as part of the present project [3]. The literature study identified numerous methods for the calculation of flame heights, incident radiation towards neighbouring buildings using different view factor methods, considering windows on the sides etc. None of these methods consider large openings in the ceiling.

In the following analysis of the model scale tests, the focus is on flame heights and incident radiation measured using two different technologies: a traditional method and one simple and robust method. Correlations presented in the literature study for the calculation of flame heights, incident radiation using point source or view factor method are compared to the experimental data. The aim is to investigate the accuracy of these methods when one is considering large openings in the ceiling. Out of a total of ten tests performed, nine were carried out with flames emerging from ceiling opening and one with flames coming out of a long side window, simulating a scenario found to be most common in the literature.

2 Theoretical aspects

2.1 Scale modelling

SP Fire Technology has over the years performed a number of studies on fire-extinguishing properties of different commodities, mainly using the so-called commodity classification method, which has provided a significant amount of knowledge concerning the initial fire development of a variety of goods [4-6]. SP has also undertaken several research projects on the effect of the rack storage geometry on the initial fire development [7-9]. These projects have included experiments both in full scale and model scale. Most recently, SP conducted a series of model tests where the fire spread from the initial fire to nearby pallet racking was investigated [10]. In the same project, the effect of room size on fire development and the risk of fire spread between low-stacked commodities was studied. Experience from these BRANDFORSK projects was of great benefit in the present project.

There are limitation in the usability of model scale testing as a research tool. The main limitation is the modelling of thermal properties of materials (enclosing surfaces and fuel) and radiation effects. Since both the thermal material properties of the enclosing surfaces and radiation effects in space are two of the most important parameters in the case of flashover, it may seem paradoxical to use scale models. In scale modelling research it is, however, often the fundamental behaviour and not the absolutely correct scale modelling of all behaviour that is important.

SP Fire Technology has a long experience of using scale models and these studies have clearly illustrated the many advantages of using scale models. SP has, for example, used scale models for fires in rack storage [10], fires on ferries [11], road tanker fire [12], reconstruction of the discotheque fire in Gothenburg [13] and in particular for tunnels [14-20]. These projects have demonstrated that the results obtained using scale models correlate well with results from full-scale trials where such a comparison has been possible. Due to the logistical difficulties associated with extremely large scale tests (and their cost), the use of scale models has been chosen as a suitable vehicle for the investigations conducted within this project.

2.2 Scaling laws

When using scale modelling it is important that the similarity between the full-scale situation and the scale model is well-defined. A complete similarity involves for example both gas flow conditions and the effect of material properties. The gas flow conditions can be described by a number of non-dimensional numbers, e.g. the Froude number, the Reynolds number, and the Richardson number. For perfect scaling, all of these numbers should be the same in the model-scale model and in the full-scale case. This is, however, in most cases not possible and it is often enough to focus on the Froude number:

$$Fr = \frac{u^2}{gL} \quad (1)$$

where u is the velocity, g is the acceleration of gravity, and L is the length. This method, often referred to as Froude scaling, has been used in the present study, i.e. the Froude number alone has been used to scale the conditions from the large scale to the model scale and vice versa. Information about scaling theories can be obtained for example from references [21-24]. In Table 2.1 the scaling of the most important parameters for this study using this method is presented.

Table 2.1 A list of scaling correlations for the model tunnel.

Type of unit	Scaling model
Heat Release Rate, HRR (kW)	$\dot{Q}_F = \dot{Q}_M \left(\frac{L_F}{L_M} \right)^{5/2}$
Time (s)	$t_F = t_M \left(\frac{L_F}{L_M} \right)^{1/2}$
Energy (kJ)	$Q_F = Q_M \left(\frac{L_F}{L_M} \right)^3$
Heat Flux (kW/m ²)	$q''_F = q''_M \left(\frac{L_F}{L_M} \right)^{1/2}$
Temperature (K)	$T_F = T_M$

a) Index M corresponds to the model scale and index F to the full scale ($L_M=1$ and $L_F=10$ in the present case).

2.3 Calculation of incident heat radiation

There are numerous methods available to calculate the incident radiation towards an object at a certain distance from the burning building. These methods vary in complexity and accuracy. Mudan and Croce give a good overview of the methods available [25]. Here, two different methods are presented, one simple and one more complicated, although relatively simple from an engineering point of view.

The first model is a point source model, assuming that the flame can be represented by a small source of thermal energy, that the energy radiated from the flame is a specified fraction of the energy released during combustion and that the thermal radiation intensity varies proportionately with the inverse square of the distance from the source. Expressed mathematically, radiant intensity at any distance from the source is given by [25]:

$$\dot{Q}_{rad,in}'' = \frac{\chi \dot{Q}_{comb}}{4\pi L^2} \quad (2)$$

where $\chi = \frac{\dot{Q}_{rad}}{\dot{Q}_{comb}}$ is the fraction of total heat release (comb) that is radiated away and L is

the distance from the flame centre to observer in m. This means the distance L is dependent on the flame height. Mudan and Croce say that while the model is elegant in its simplicity, two important limitations should be recognized. The first limit involves the modelling of radiative output and the second is the description of the variation of the intensity as a function of the distance from the source. There is a considerable variation in the fraction of radiated energy from flames. A value that is often quoted is 30 % ($\chi = 0.3$) for many fuels [26].

The second model is a solid flame radiation model. The solid flame model is based on the proposition that the entire visible volume of the flame emits thermal radiation and the non-visible gases do not emit much radiation. The thermal radiation intensity, $\dot{Q}_{rad,in}''$, can be obtained using the following equation [25]:

$$\dot{Q}_{rad,in}'' = \tau \cdot E_f \cdot \phi \quad (3)$$

where τ is the atmospheric transmissivity (set equal to 1 here), E_f is the average emissive power of the flame and ϕ is the geometric view factor which is a measure of the decrease of the radiation at different distances. Siegel and Howel gives an expression for the configuration factor of a rectangular radiator and a remote receiver, see equation (4) [27]:

$$\phi = \frac{1}{2\pi} \left[\frac{x}{\sqrt{1+x^2}} \tan^{-1} \left(\frac{y}{\sqrt{1+x^2}} \right) + \frac{y}{\sqrt{1+y^2}} \tan^{-1} \left(\frac{x}{\sqrt{1+y^2}} \right) \right] \quad (4)$$

where

$$X = H_f/r$$

$$Y = W_f/r$$

H_f =height of rectangular (m)

W_f =width of rectangular (m)

r =distance between radiating and receiving surface (m).

Equation (4) determines the configuration factor in one of the corners of a rectangle representing the flame volume. The distance r must be at right angles to the rectangle. Configuration factors are additive given the configuration factors of each contributing part are calculated from the same receiver [28]. The total configuration factor ϕ is a sum of the configuration factors of each rectangle. The emissive power of a large turbulent fire may often be approximated by the following expression [25]:

$$E_f = E_b \cdot \varepsilon \quad (5)$$

where E_b =blackbody emissive power, kW/m², and ε is emissivity. The emissive power can vary considerably depending on the fuel type and the diameter of the flame volume. If the mean radiation temperature of the fire is known it can be converted to irradiance using the Planck's law of radiation. Thus, the blackbody emissive power, E_b is given by [25]

$$E_b = \sigma (T_f^4 - T_a^4) \quad (6)$$

where

T_f =radiation temperature of flame, K

T_a =ambient temperature, K

σ =Stefan-Boltzmann constant, kW/m²K⁴

2.4 Flame height

The flame height can either be estimated from the visual observations or by calculations. Heskestad derived the following formula [29]:

$$H_f = -1.02D + 0.235\dot{Q}^{2/5} \quad (7)$$

Equation (5) applies well for pool fires and has been validated for rack storages and other types of fuels [30]. This equation has, however, not been applied for flame heights in buildings with large openings in the ceiling.

During the Kuwait war in early 90s, numerous jet fires were created as a consequence of the war. These fires has been analysed by Evans *et al.* [1994]. The heat release rates and flame heights were estimated to vary between 0.1 - 2 GW and 20 - 70 m, respectively. The flame height correlations was found to be as follows:

$$H_f = 0.21 \cdot Q^{2/5} \quad (8)$$

where Q is in kW. The diameter of the fuel source is not important here as the diameter is very small in relation to the flame height. Except for the diameter dependence of the fire source, this equation is very similar in form as the one given by Heskestad on pool fires in the open. These equations will be used in the analysis of the experimental data presented later in this report.

A relevant paper to this study was presented by [31] on reduced-scale mass fire experiments. In that paper Heskestad discusses low flame-height data exhibiting the transition from coherent flaming to distribute flamelets when the ration H_f/D became smaller than about 0.5. This is very interesting when concerning industrial buildings, where the flame heights may be low compared to the diameter of the fire base (flame through openings in the ceiling). When this transition occurs, the air induced or entrained by combustion, if shared by all the fuel vapours, would dilute the vapours below their ability to burn. From these consideration the author speculates that mass fire in sufficiently large homogenous fuel beds may only be possible as distributed localized fires. Experiments carried out by Heskestad using wood fibreboards arranged to produce a square array measuring 7.32 m on the side, showed actually that luminous flames showed first tendencies of breaking up into distribute flamelets near $H_f/D = 0.52$, being fully broken up near $H_f/D = 0.34$. These numbers are very interesting for the purpose of the investigation carried out here. As the opening becomes too large, the flames may break up into smaller fires. Heskestad was able to go down to $H_f/D = 0.04$ in his experiments where the entire burner surface showed flickering blue flamelets racing back and forth.

2.5 Heat flux measurements

The plate thermometer (PT) was developed by Wickström in the 80s for controlling fire resistance furnaces to obtain harmonized test results throughout Europe [32]. At that time the PT was not thought to be a heat flux meter but to measure an ‘effective temperature’ assuring the same heat transfer to specimens in various types of fire resistance furnaces [33]. The PT has since then been specified in the relevant international (ISO 834) and European (EN 1363-1) standards. The PT consists of a stainless steel plate, 100 mm × 100 mm and 0.7 mm thick, with a 10 mm thick insulation pad on the backside.

Heat Flux Meters (HFM) such as Gardon or Schmidt-Boelter (SB) gauges are used routinely in fire tests to measure total heat flux by radiation and convection. They measure total heat flux to a water cooled small surface. When the cooling water temperature is kept near the ambient gas temperature, the heat transfer by convection will be reduced to negligible levels and the probe will measure very close to incident radiant heat flux.

Ingason and Wickström [34] were able to demonstrate that the PT could be used as a HFM meter. For the project presented here this is of great interest as we can use PT instead of HFM to measure the heat flux to neighbouring buildings. In this project some effort has been made to compare both these methods, mainly in order to see whether they are applicable to the applied situation and as a further proof of the applicability of the measuring method using PT instead of HFM. Ingason and Wickström developed a calculation method to calculate the heat flux from a PT. The incident heat flux by radiation can be derived from the PT temperature as:

$$\dot{q}''_{inc} = \frac{\varepsilon_{PT} \sigma T_{PT}^4 + (h_{PT} + K_{cond})(T_{PT} - T_{\infty}) + \rho_{st} c_{st} \delta \frac{\Delta T_{PT}}{\Delta t}}{\varepsilon_{PT}} \quad (9)$$

Where c is the heat capacity [J/kg/K], h the convective heat transfer coefficient [W/m²/K], K_{cond} a conduction correction factor [W/m²/K], \dot{q}''_{inc} incident heat flux by radiation [W/m²], T temperature [K], t time [s], ε surface emissivity [-], δ thickness of steel plate [m], σ Stefan-Boltzmann constant [W/m²/K⁴] and ρ density [kg/m³]. The best fit between all the tests in the Arvidson and Ingason study [35] was obtained for conduction correction factor $K_{cond}=22$ W/m²/K. In the calculations the following values have been used: $\varepsilon_{PT} = 0.8$, $h_{PT} = 10$ W/m²/K, $\rho_{st} = 8100$ kg/m³, $c_{st} = 460$ J/kg/K, and $\delta = 0.0007$ m.

Equation 9 was further developed by Häggkvist [36] and he derived the following equation:

$$\left[\dot{q}''_{inc} \right]^{i+1} = \frac{\varepsilon_{PT} \sigma [T_{PT}^4]^i + (h_{PT} + K_{cond})([T_{PT}]^i - T_{\infty}) + C_{heat,\beta=1/3} \frac{[T_{PT}]^{i+1} - [T_{PT}]^i}{[t]^{i+1} - [t]^i}}{\varepsilon_{PT}} \quad (10)$$

The equations are very similar to each other even if in Equation (10) the exact order of calculation is defined. The main difference is the value of K_{cond} , which in the work by Häggkvist was estimated to be 8.43 W/m²/K, and the lumped heat capacity coefficient $C_{heat,\beta=1/3} = 4202$ J/m²/K. In Appendix 2, Equation (10) was used to calculate the radiation from the PT measurements.

3 Experimental set-up

The tests were performed by creating a fire inside a scale model of an industrial building. The scale used was assumed to be 1:10. Measurements were performed both inside and outside the model to observe the conditions and to assess the heat exposure and risk for fire spread at different distances from the building (or the model in our case).

3.1 Scale-model of industrial premises

A model of an industrial building was constructed at SP and placed beneath the industrial calorimeter [37-38]. The model was 6 m long, 3 m wide and 0.7 m high (see Figure 3.1, Figure 3.2 and Figure 3.3). The model was constructed with 10 mm Promatect boards. To protect the construction the ceiling was covered by 50 mm insulation with an aluminium sheet facing the inside of the enclosure. The walls and floor were covered by 20 mm insulation.

In each short wall there was a centred opening at the floor, $0.8 \text{ m} \times 0.4 \text{ m}$. These openings was closed, partly open (half) or open, and different combinations of these openings were used during the test series (see Table 4.1). In the ceiling there were four ventilation opening ($0.15 \text{ m} \times 0.15 \text{ m}$). These openings (V1 – V4 in Figure 3.2) were always open and represented 0.5 % of the ceiling area. Part of the ceiling was constructed so that different larger ceiling openings could be obtained. This was done to simulate the fire burning through the ceiling. Three different sizes of the ceiling opening were used as signified by the dotted and dashed lines in Figure 3.2. In all cases the opening was 1.5 m wide. In the first case the opening was 0.6 m long (corresponding to 5 % of the full ceiling area), in the second case the opening was 1.8 m long (corresponding to 15 % of the full ceiling area) and in the final case the opening covers the full 3 m breadth of the ceiling (corresponding to 25 % of the full ceiling area). In one case, however, a 5 % opening was centred in the ceiling. This is not illustrated by the figure. Furthermore, in one case there was no ceiling opening (except the four ventilation openings), but instead an opening in the wall towards the radiation measurements (see Figure 3.1). This opening was $0.3 \text{ m} \times 3.0 \text{ m}$, which corresponds to the 5 % of the ceiling area.

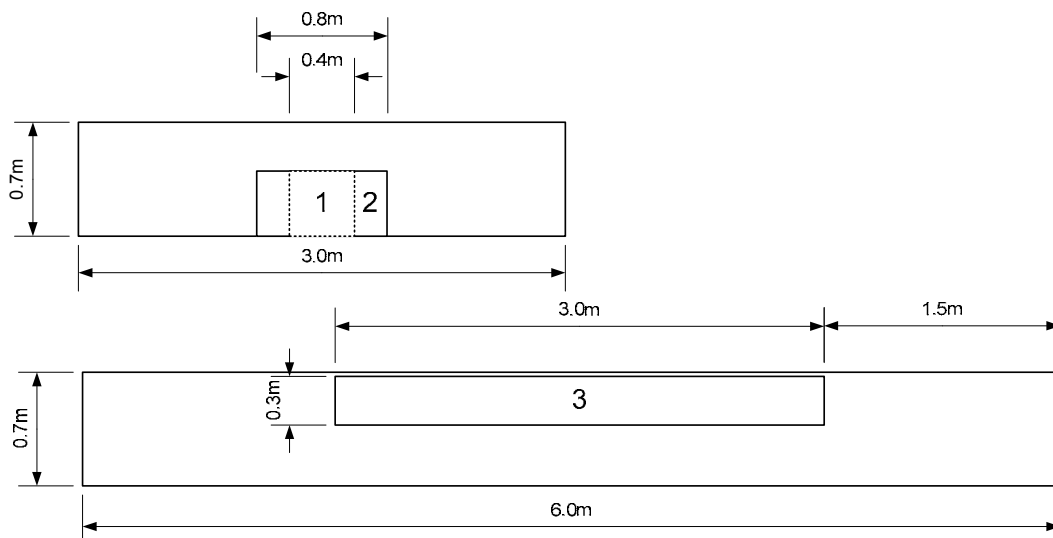


Figure 3.1 Side view of the experimental set-up. Opening 1 represents an industrial port, while opening 2 represents a double port. Opening 3 simulates a window or opening in the upper part of the wall.

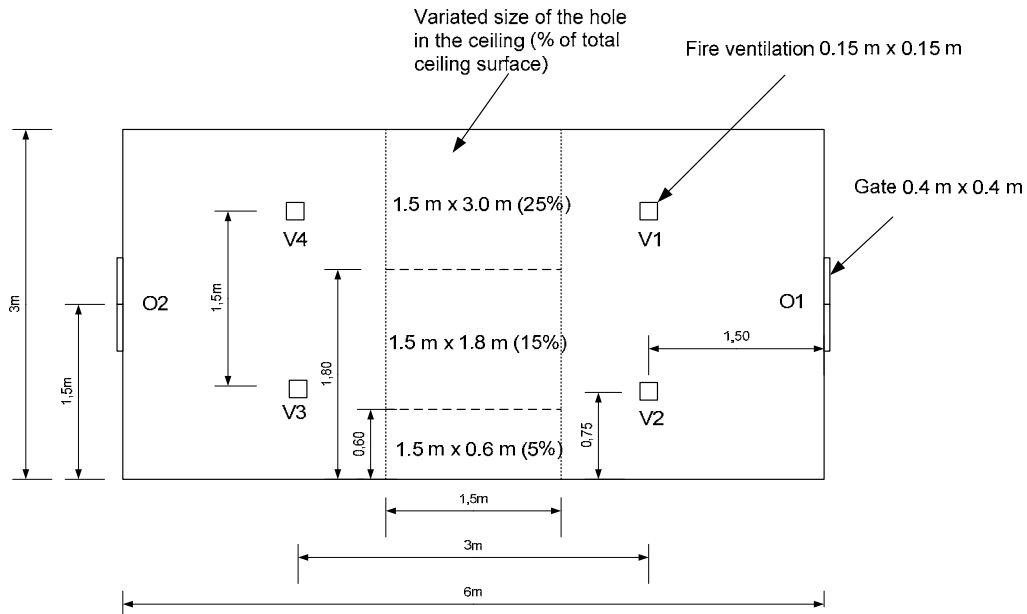


Figure 3.2 Top view of the experimental set-up of the scale model. V1 to V4 are fire ventilation openings in the ceiling. O1 and O2 are openings in the short walls, 2 m × 0.4 m × 0.4 m on each side.



Figure 3.3 Photo from the inside of the model-scale compartment.

3.2 Measurements

The main purpose of the test series was to study the variation in heat fluxes towards an imagined neighbouring building. Therefore, the heat flux from the fires was measured using two different types of sensors: heat flux meters and plate thermometers. Heat flux meters were positioned in three directions from the fire (see Figure 3.4). In total ten heat flux meters were used. These were calibrated for a maximum heat flux of between 10 kW and 100 kW, depending on the measurement position. In three positions plate thermometers were also used. For reference, thermocouples were added to measure gas temperatures in the same positions as for the plate thermometers (see Figure 3.4). The height of these measurement positions was 25 cm above the inner surface of the ceiling of the model-scale compartment. This was 178.5 cm above the floor of the fire hall.

Gas temperatures were also measured with thermocouples in numerous positions inside the scale model. This was done to study fire development and temperature distribution during the different tests. In total 12 thermocouples (TC) were used: six in a TC tree from the ceiling between the openings V1 and V2, with a distance of 0.1 m between each TC; one TC in the ventilation opening V1; and five along the centreline 10 cm below the ceiling (see Figure 3.4)

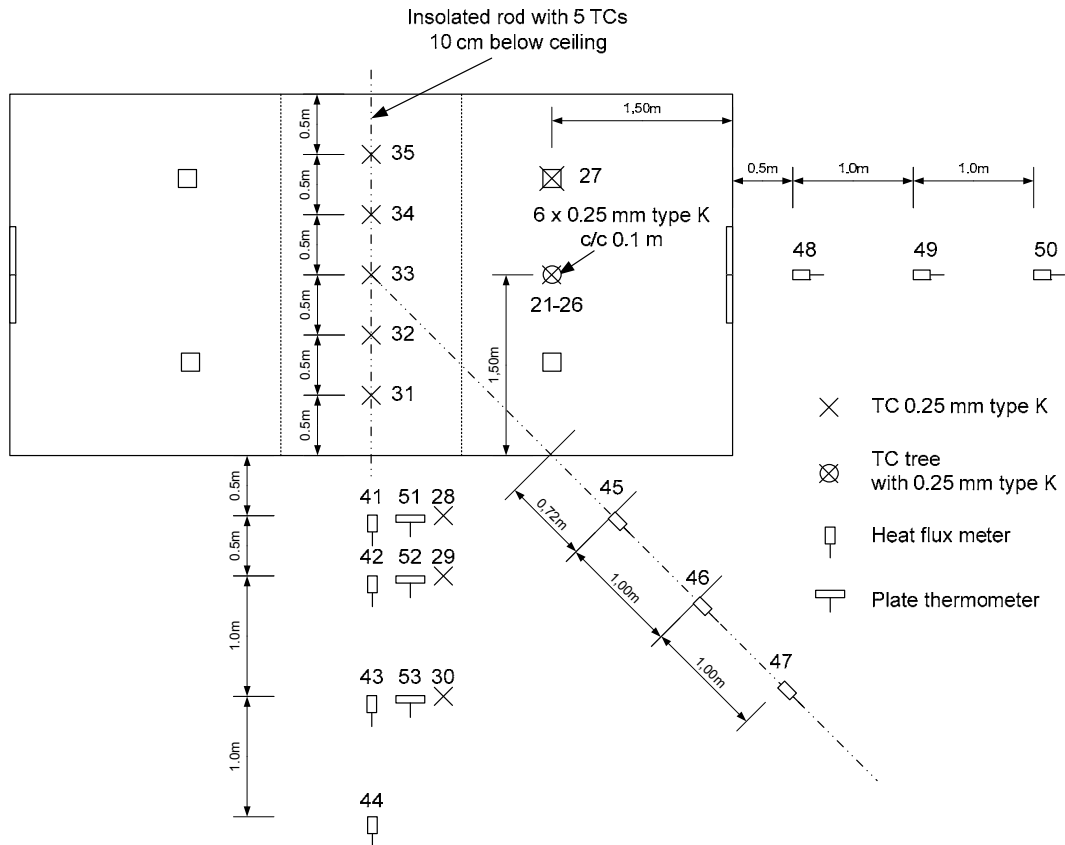


Figure 3.4 Positions of measurement sensors, including channel numbers.



Figure 3.5 Photo with the scale model, flames from the ceiling opening, the height ruler, and the hood collecting the exhaust gases.

The fire development was also registered by measuring the heat release rate. This was done by collecting the fire gases in a hood/exhaust system and then using oxygen calorimetry [39-40]. The factor E used in the calculations is described in Section 3.3.

During the test series, velocity measurements of the flow through the openings O1 and O2 were made using a hand held velocity meter. The results of these measurements are presented together with the test protocols in Appendix 1. Estimations of the flame heights are also given in Appendix 1. A height ruler was made and mounted on the scale model to facilitate this estimation (see Figure 3.5).

3.3 Fuel

Wood cribs with ribs made out of fir (*pinus silvestris*) were used as fuel in the tests. Two different sizes of wood cribs were used: wood crib 1 with 2.1 m long sticks and wood crib 2 with 2.7 m long sticks (see Figure 3.6, Figure 3.7 and Figure 3.8). The amount of fuel, outer dimension, and spacing between the stick were selected to simulated a distributed fire source that could burn for a suitable period of time. Both wood cribs were constructed using four layers with 12 sticks in each. Two additional sticks were used to raise the wood crib a distance above the floor making it possible to place four pools with heptane (35 cm × 35 cm) beneath the wood crib (see Figure 3.7). The pools with heptane were used to ignite the wood cribs, but also increased the total fire size. The average mass of nine wood cribs of type 1 used in the test series was 80.8 kg and the mass of wood crib 2 used in Test 7 was 105.4 kg. The average density of the wood in the cribs was approximately 530 kg/m³. A volume of 2.5 L of heptane was used in each pool, giving a total of 10 L heptane in each test.



Figure 3.6 Photo of wood crib 1.

The HRR from wood is dependent on the water content of the wood. This means that when calculating the HRR, the water content needs to be considered. During the fire tests, both wood and heptane were burning, at least until the heptane is consumed. It is difficult to determine what part of the HRR can be assigned to wood and what part to heptane, respectively. If a combustion enthalpy of 18 MJ/kg is assumed for dry wood, this corresponds to a E factor of 14.05 MJ/kg O₂. The E factor of heptane is 12.69 MJ/kg O₂. An E factor of 12.69 MJ/kg O₂ for wood corresponds to a water content of approximately 8.5 %. This value is probably somewhat lower than the real average water content. The heptane probably contribute to a large part during the most important or interesting part of each test and therefore this value has been used as an average value for the E factor. For wood this corresponds to a combustion enthalpy of 16.3 MJ/kg.

In Figure 3.9 the HRR curve is presented for wood crib 1 freely burning beneath a calorimeter, i.e. not inside the model scale building. A free burn test of wood crib 2 was not carried out.

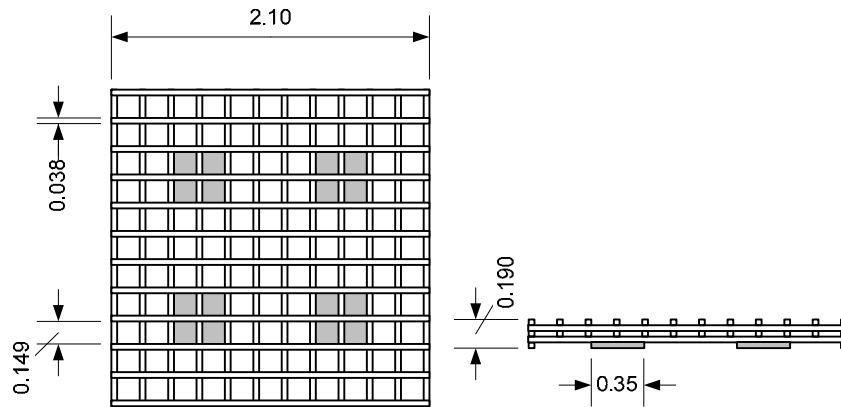


Figure 3.7 Dimensions of wood crib 1 and position of the four heptan pools (Dimensions in m).

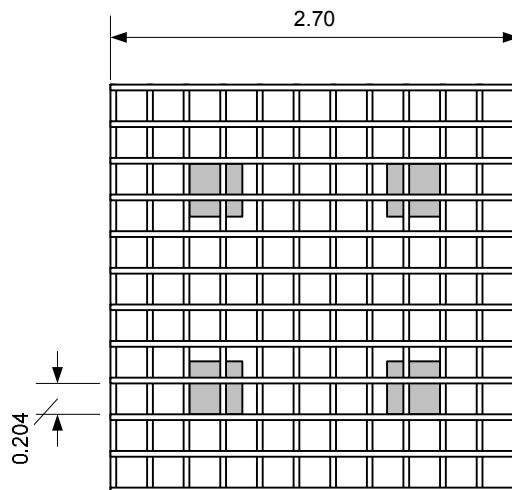


Figure 3.8 Dimensions of wood crib 2 and position of the four heptan pools (Dimensions in m).

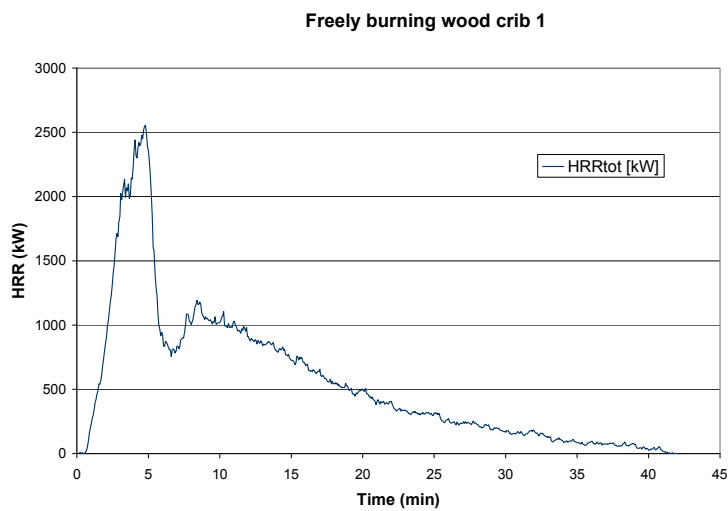


Figure 3.9 HRR for wood crib 1 freely burning under a calorimeter.

The energy content in the fuel for each test is given in Table 5.1 together with the total heat released.

4 Experimental procedure

As the aim of the test series was to study the radiation effect of the openings in the ceiling and in the wall, the fire source itself was not altered during the test series. However, for reference a larger fire source (wood crib 2) was used in one of the tests. The fire source was always positioned centred on the floor (see also Section 3.3). The main variations during the test series were the different openings and positions. The two openings O1 and O2 acted in most of the test as inlet air openings. However, in Test 1 and Test 2 there were no other openings (except the small ventilation opening V1-V4), which means that all air and gas flow were through these openings. Two different combination were used: one with only half of O1 open (and O2 closed) and the second with both openings fully open. This corresponds to one or four 4 m × 4 m industrial gates in real scale. The main variation during the test series was the openings simulating the fire burned through the ceiling or the upper part of one of the long walls. The different sizes of the ceiling openings used corresponded to 5 %, 15 % and 25 % of the total ceiling area. The opening in the wall had the same area as the smallest ceiling opening. The test conditions are summarized in Table 4.1.

Table 4.1 Summary of the test series.

Test id	Wood crib	O1 (m ²)	O2 (m ²)	Ceiling opening (%)	Wall opening
1	1	0.16	0	0	No
2	1	0.32	0.32	0	No
3	1	0.32	0.32	5	No
4	1	0.32	0.32	15	No
5	1	0.32	0.32	25	No
6	1	0.16	0	5	No
7	2	0.32	0.32	5	No
8 ^{a)}	1	0.32	0.32	5	No
9	1	0.32	0.32	5 (centred)	No
10	1	0.32	0.32	0	Yes

a) Repetition test of Test 3.

For the ignition of the heptane pools in Test 1 - Test 3, an electronic ignition device was used. Since this method was not considered totally reliable, from Test 4 the pools were ignited manually (Appendix 1). After ignition of the heptane pools the fire spread to the wood crib and the fire was then let to burn until it self-extinguished. After the test, any remaining fuel and ashes were weighed to calculate the consumed mass.

5 Results

In this chapter results for different parameters are presented. The chapter is focused on comparisons between tests and comparisons between measurements and calculations. Detailed results from each test are given in Appendix 2, which show a detailed time-resolved results of the measurements. Test 3 can be regarded as representing a reference scenario for the test series and therefore many results are compare to the corresponding results for Test 3, while other comparisons are only presented for Test 3.

5.1 Heat release rate

Firstly, the heat release rate (HRR) is enhanced compared to the free burning test (2555 kW) shown in Figure 3.9. This increase varies depending on the ventilation openings, but for test 3 it is 15 % (2930 kW) and 44 % for test 4 which resulted in the highest HRR (3680 kW) using wood crib 1. This is mainly due to re-radiation from the surrounding walls and is in line with observations obtained from other studies [41-42].

The sizes and positions of the openings affect the fire development and thereby the HRR. In Figure 5.1 a comparison for cases with and without ceiling openings is presented. The effect of the ceiling opening on the fire development is very apparent. A smaller difference, but still significant, can be seen for cases with ceiling opening, but different sizes of the inlet openings (see Figure 5.2). However, if the only difference is the size of the ceiling opening, the effect on the HRR-curve is even smaller. The main difference is the maximum HRR and the shape of the curve near the time for the maximum (see Figure 5.3). The highest HRR is actually reach in Test 4 with 15 % ceiling opening.

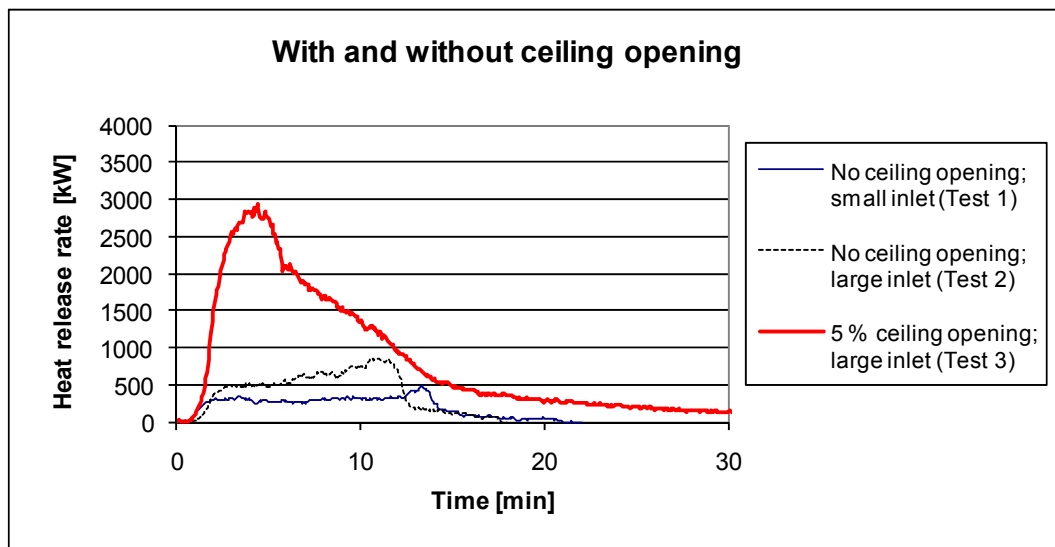


Figure 5.1 HRR curves for tests with a) one small inlet opening (0.16 m^2) and no ceiling opening (Test 1), b) two large inlet openings ($2 \times 0.32 \text{ m}^2$) and no ceiling opening (Test 2), and c) two large inlet openings ($2 \times 0.32 \text{ m}^2$) and a 5 % ceiling opening (Test 3).

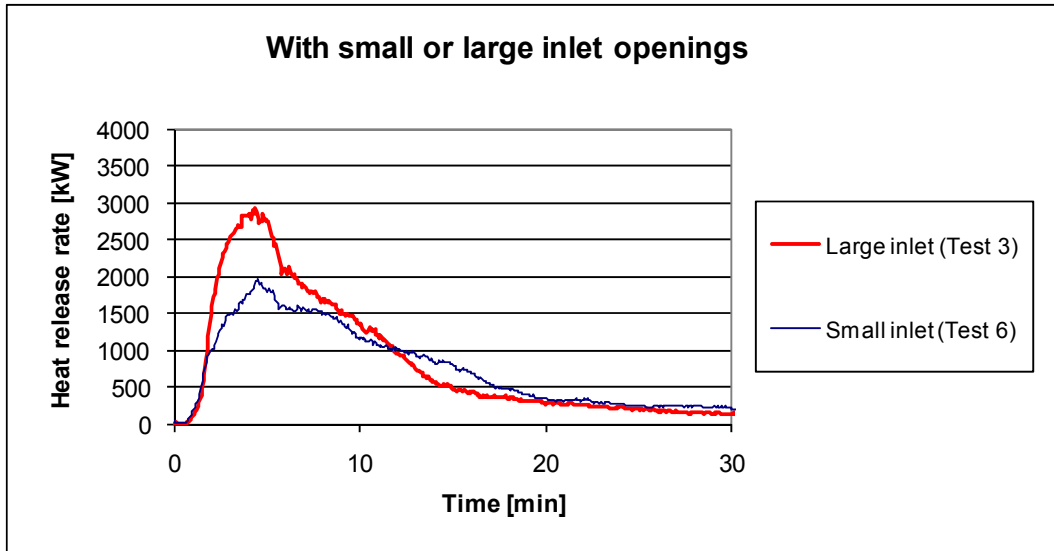


Figure 5.2 HRR curves for tests with large ($2 \times 0.32 \text{ m}^2$; Test 3) and small (0.16 m^2 ; Test 6) inlet openings, respectively. Both tests had a 5 % ceiling opening.

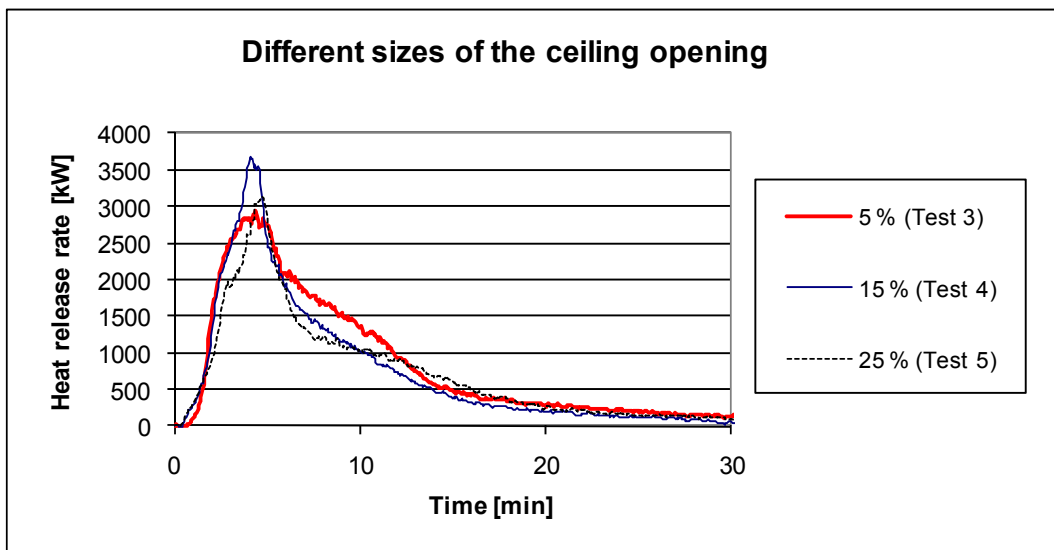


Figure 5.3 HRR curves for tests with a) 5 % ceiling opening (Test 3), b) 15 % ceiling opening (Test 4), and c) 25 % ceiling opening (Test 5). In all three tests, the inlet openings were $2 \times 0.32 \text{ m}^2$.

The aim of the project was not to study the fire behaviour inside the compartment, but in one of the tests a wood crib larger than the reference crib was used and the HRR-results due to this variation is presented in Figure 5.4. The larger wood crib leads to higher HRR, but only during the first part of the tests. From five minutes after ignition the curves are similar to each other.

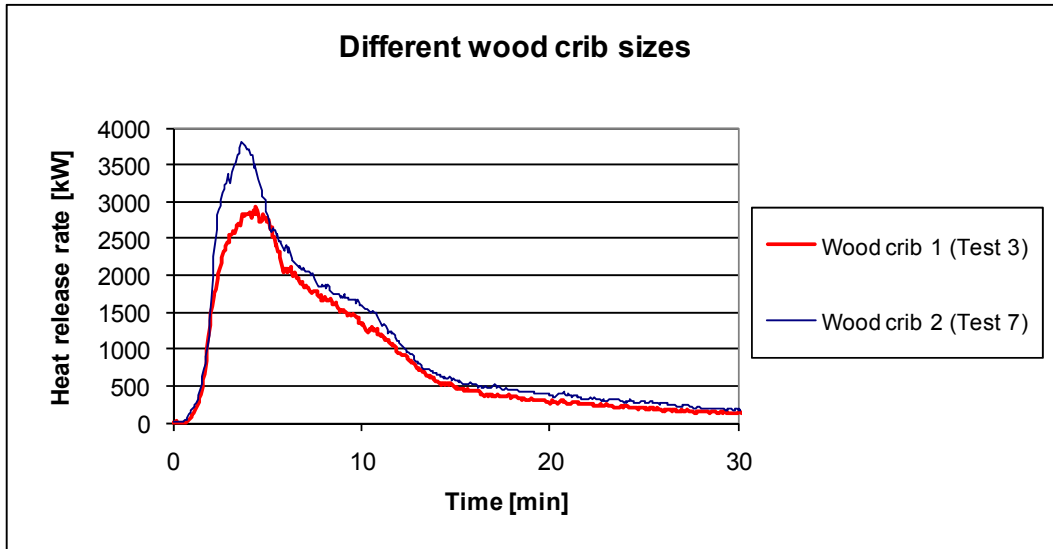


Figure 5.4 HRR curves for tests with two different wood crib sizes: reference case (Wood crib 1; Test 3) and a larger wood crib (Wood crib 2; Test 7).

An important characteristic that influences the fire behaviour is the position of the opening. In Figure 5.5 HRR curves for three tests with the same sized opening with different position are presented. The highest HRR was obtained with a centred ceiling opening and the lowest HRR was obtained with a wall opening instead of a ceiling opening.

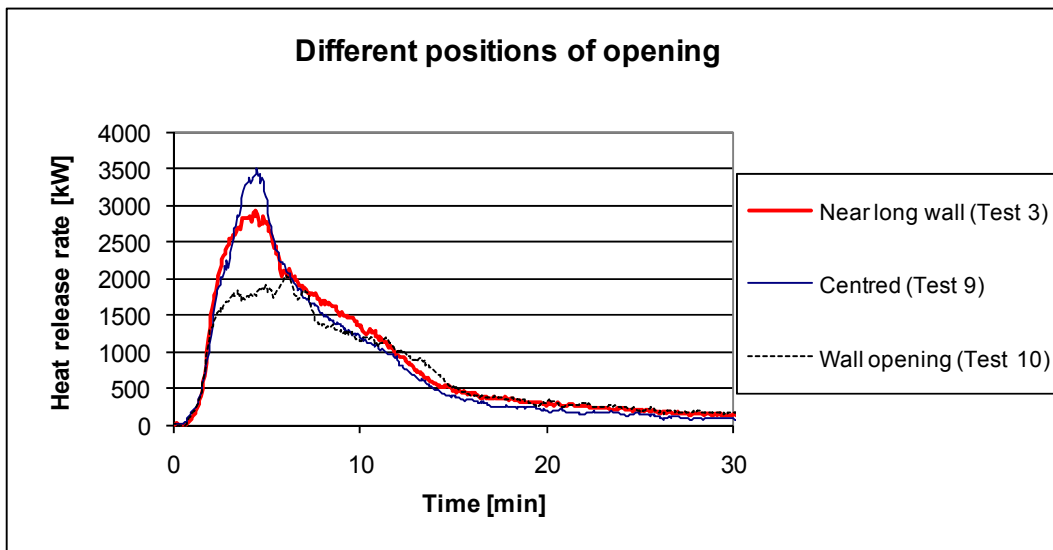


Figure 5.5 HRR curves for tests with the same opening size (5%), but different positions: a) in the ceiling near one of the long walls (Test 3), b) centred in the ceiling (Test 9), and c) as a wall opening (Test 10).

Figure 5.6 is included to show the repeatability of the HRR from one test to another when the same test conditions are used. The tests were performed with a 5% ceiling opening near one of the long walls and as can be seen the repeatability is good.

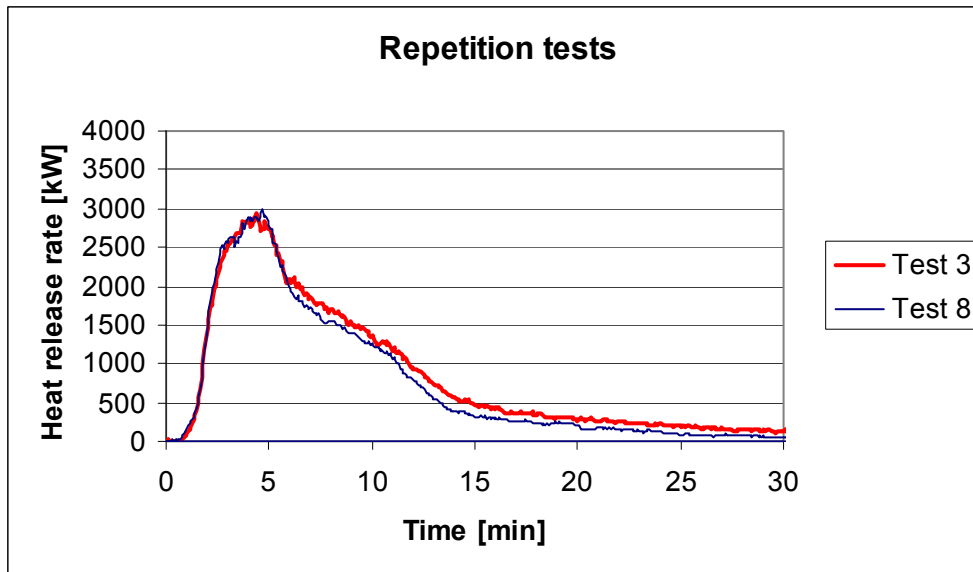


Figure 5.6 HRR curves for tests with the same conditions (repetition tests), i.e. 5 % ceiling opening near one of the long walls.

In Table 5.1, a summary of the original energy content of the fuel and the total energy consumed of wood crib and heptane during the test is given. The values are based on integration of HRR curves and weight of the fire debris after each test.

In Table 5.2 the maximum HRR and the time to maximum HRR are presented for each test. If there were no ceiling openings, the maximum possible HRR inside the enclosure is 150 kW for the case with only a small O1 (0.16 m²) and 610 kW for the case with O1 and O2 fully open (0.64 m²). During the relatively steady period between 8.5 min and 11.5 min in Test 1, the average HRR was 311 kW. In both Test 1 and Test 2, flames exited opening O1. This occurred at 12:30 for Test 1 and at 4:28 for Test 2. At these times the HRR was approximately 320 kW and 500 kW, respectively. Flames exited also the ventilation holes in the ceiling (see Appendix 1) and this was observed at the first time at approximately 3:04 for Test 1 and 1:52 for Test 2. In Figure 5.7 an example of flames out through openings during Test 2 is given.



Figure 5.7 Flames out through openings during Test 2.

Table 5.1 Energy content of the fuel consumed and the total heat released.

Test no	Original mass wood (kg)	Consumed wood (kg) ^{a)}	Consumed heptane (kg) ^{a)}	Q_{fuel} (MJ) ^{a), b)}	Q_{HRR} (MJ)	$Q_{\text{HRR}}/Q_{\text{fuel}}$
1	84.04	14.94	5.95	509	216	0.43
2	85.46	30.8	6.84	809	341	0.42
3	83.88	83.3	6.84	1660	1570	0.95
4	76.46	75.74	6.84	1540	1380	0.90
5	79.12	78.52	6.84	1580	1380	0.87
6	76.22	75.60	6.84	1540	1580	1.03
7	105.42	104.82	6.84	2010	1940	0.96
8	77.88	77.28	6.84	1560	1380	0.88
9	83.24	82.46	6.84	1650	1450	0.88
10	80.64	79.32	6.84	1600	1410	0.88

a) The values correspond to the fuel consumed during the test, not the original mass of fuel.

b) A heat of combustion of 16.3 MJ/kg has been used for wood and 44.56 MJ/kg for heptane.

Assuming that the scale factor for the tests is 1:10, we can multiply the time by 3.16 and the HRR with 316. In Table 5.2 a summary of all maximum HRR and the time to reach them is presented. The values have also been converted to a full scale values in order to compare to large scale.

Table 5.2 Maximum HRR in the model scale tests. For comparison, the corresponding maximum HRR full scale is included.

Test no	Time to HRR_{max} (min)	HRR_{max} (kW)	Time to $\text{HRR}_{\text{max, full scale}}$ (min)	$\text{HRR}_{\text{max, full scale}}$ (MW)
1	13.3	483	42.2	153
2	10.5	857	33.3	271
3	4.40	2930	13.9	927
4	4.07	3680	12.9	1165
5	4.73	3150	15.0	995
6	4.53	1960	14.3	619
7	3.60	3810	11.4	1204
8	4.67	2980	14.8	943
9	4.47	3490	14.1	1105
10	6.00	2040	19.0	646

In summary, the effects of the building on the heat release rate are clearly shown by these experiments. Compared to free burning conditions, the maximum HRR is increased by 14 % with 5 % opening in the ceiling and increased by 40 % for the case when the ceiling opening covered 15 % of the ceiling. It is interesting to note is that if the opening gets larger, some of the re-radiation effects are reduced and the HRR is reduced. The effects are clearly dependent on the location and the size of the openings. With the openings in the ceiling the HRR become larger than when the opening is along the wall and it becomes larger if the opening is located centrally in the building rather than closer to the wall. This can be explained by the possibility of the fresh air coming in through the inlet openings to access the combustion area. When the openings are in the ceiling the fresh air entrainment is more symmetrical compared to when the air can only access from one side. Further, when there are only small openings in the ceiling the fire becomes ventilation controlled. The highest HRR are then only about one third of the free burn HRR.

5.2 Temperature

The gas temperatures inside the model building are dependent on the HRR and the openings. In Appendix 2 the temperatures over the height of the model as well as in the small and large ventilation openings are presented for each test. The thermocouple tree registers the highest temperature when the large openings are closed. Higher temperatures are observed with the larger inlet opening compared to the smaller one. This is due to the fact the air has better access to the combustion zone with the larger inlet opening. In these tests, a wall of flame were observed just inside the model (see Figure 5.8). In Figure 5.9, the measured gas temperatures are shown for Test 2 (larger inlet opening) and only small ventilation openings in the ceiling, and Test 3 with larger inlet opening and 5 % ceiling opening. In Test 2 the highest temperatures are about 900 °C, at the ceiling and about 600 °C closer to the floor. In Test 3, the temperatures are lower as more heat is ejected through the large ceiling opening in the centre.



Figure 5.8 Flames inside the model building during Test 1.

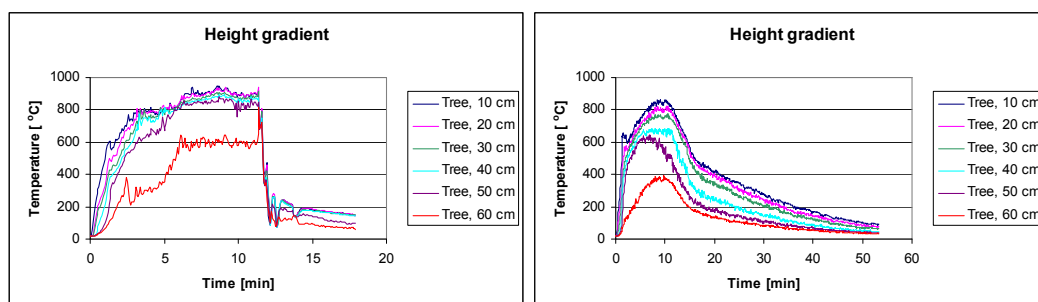


Figure 5.9 Temperature gradient inside the model building in Test 2 (left) and Test 3 (right). The temperatures were measured at elevations 0.1, 0.2, 0.3, 0.4, 0.5 and 0.6 m, respectively from the ceiling.

When the ceiling openings get larger, the gas temperature in the thermocouple tree are generally reduced, because of the stream of fresh air passing on their way to the fire source. Comparing Test 4 (15 %) and Test 5 (25 %), we see this reduction, from 850 °C to 600 °C and 500 °C respectively.

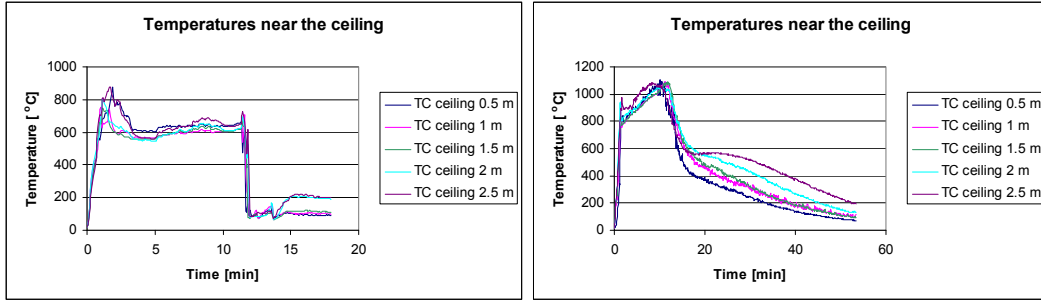


Figure 5.10 Temperature along the ceiling where the openings are located for Test 2 (left) and Test 3 (right). The distances are measured from the wall closest to the radiation measurements (see Figure 3.4).

The temperatures in the openings across the ceiling are generally around 1000 °C – 1100 °C depending on the size of the opening and the size of the fire. The differences in gas temperatures are not as pronounced as on the HRR.

5.3 Flame heights

In Appendix 1, protocols showing the flame height observations are given for each test. This information is based on the analysis of video recordings and manual observations during the tests. As the flame height is an important parameter obtained from these experiments, much effort has been put into establishing reliable data. However, this type of data is always rather subjective and may cause some uncertain results. In the flame height analysis only flame height observations for the fire development phase have been used. Observations from the decrease phase are, however, included in the protocols in Appendix 1. In order to compare the estimated flame heights, equation (7) was used to plot the data. The flame height ratio (H_f/D) was plotted as a function of $Q^{2/5}/D$ in

Figure 5.11. The effective diameter ($D_{eff} = \sqrt{\frac{4A}{\pi}}$) was used for the plot. The data is separated by the opening size in % and type of wood crib (WC1 or WC2), where WC2 is the larger one. There is a good correspondence to the correlation with a regression coefficient r equal to 0.922. The correlation can be expressed as:

$$\frac{H_f}{D} = -0.38 + 0.219 \frac{\dot{Q}^{2/5}}{D} \quad (11)$$

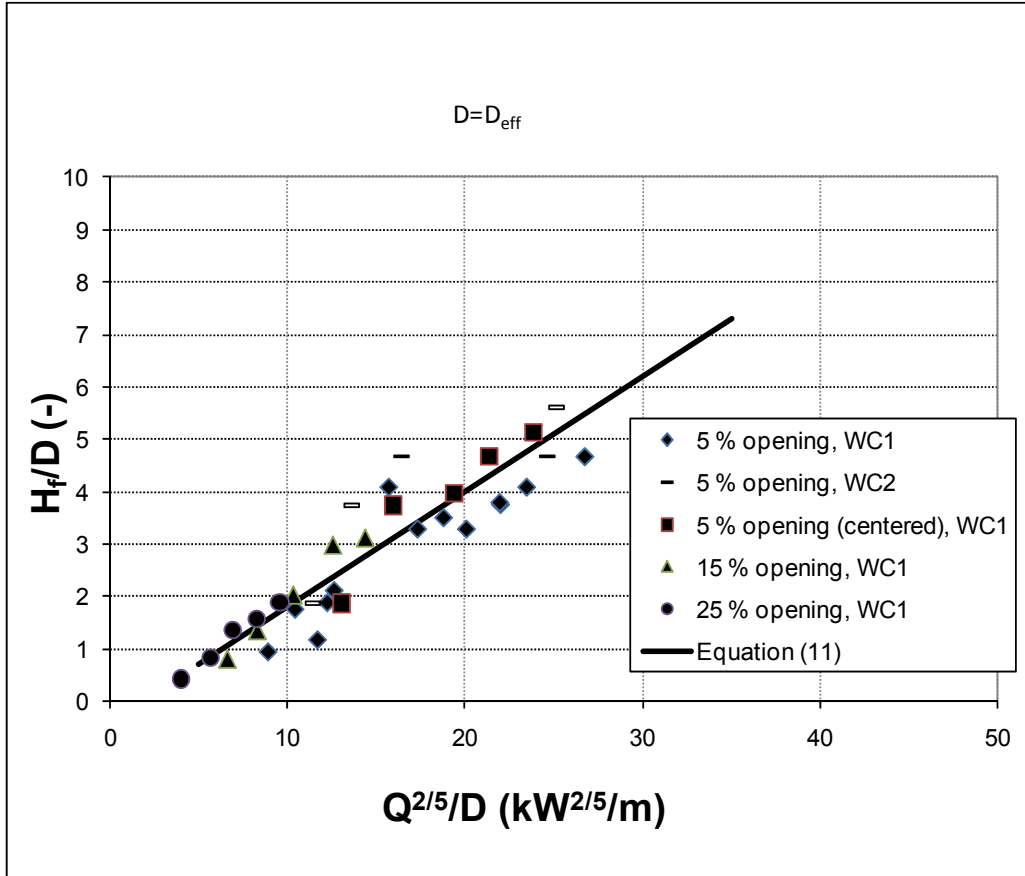


Figure 5.11 The flame height correlation based on effective diameter of the opening.

Sometimes when the fire base is very long compared to the width, it may be better to use the shorter side of the fire base. This has been done and in Figure 5.12, the data is plotted by using $D=W$, where W is the shorter side of opening. Despite the fact that the data show a very similar correspondence, we obtain a slightly better regression coefficient, or $r=0.930$. The correlation in this case becomes:

$$\frac{H_f}{W} = -0.5 + 0.21 \frac{\dot{Q}^{2/5}}{W} \quad (12)$$

The second term in the equation is the same as the one proposed by Evans for the large Kuwait jet fires (see equation 8) with the exception that Evans used the diameter instead of the width. This correlation can be used for estimating flame height in relatively large openings in industrial buildings, when using the short side of the opening as a diameter.

Another observation is that the maximum flame height ratio H_f/D is higher than 0.5 for all the tests. The maximum ratio ranged between 0.5 and 10 for the test series. This explains why we did not observe any type of break-up of the flames into smaller flames in the openings. As expected the lowest values of H_f/D was found for the larger openings (15 % and 25 %, respectively). The data based on the large fuel source, WC2, does comply relatively well with the other data.

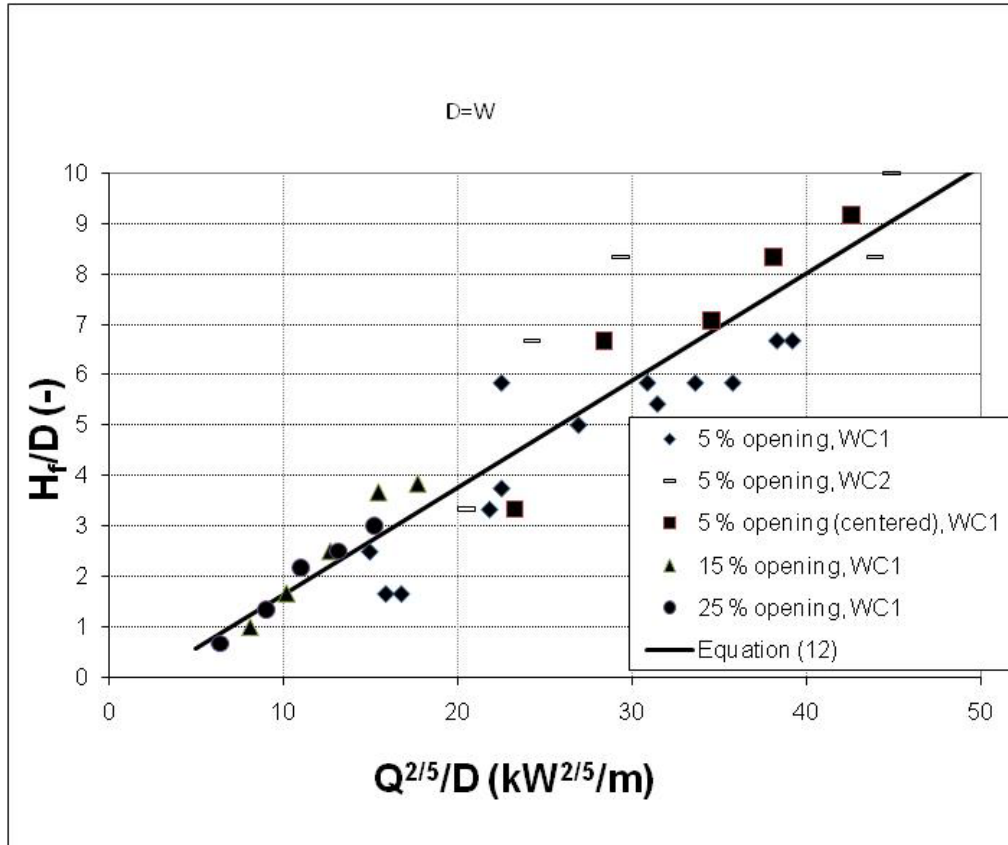


Figure 5.12 The flame height correlation based on the width of the opening.

5.4 Heat flux

Radiation and heat exposure are very important when assessing the risk for fire spread between buildings. The heat flux was in the test series measured using different methods. In Section 5.4.1 the results from measurements with heat flux meters are presented, while heat fluxes calculated from the measurements with plate thermometers are presented in Section 5.4.2.

5.4.1 Comparison of heat flux measurements

The position of the flame has a significant impact on the results of the heat flux measurements. In Figure 5.13 the heat flux results are presented for tests with different ceiling opening sizes. The heat flux results presented were measured 1 m from the long wall. It is interesting to note that the larger the opening, the lower the maximum heat flux. The explanation for this is that since the closest edge of the opening is always at the same distance from the heat flux meter, the centre of the flame is moved away from the meter when the size of the opening is increased. A similar effect can be seen in Figure 5.14 where the heat flux results for tests with the same opening size, but in different positions, are compared. The highest heat fluxes are reached for the wall opening, while the tests with the 5 % opening centred in the ceiling gave the lowest level. In Figure 5.14 the heat flux results for the repetition test (Test 8) are also included, showing the good repeatability.

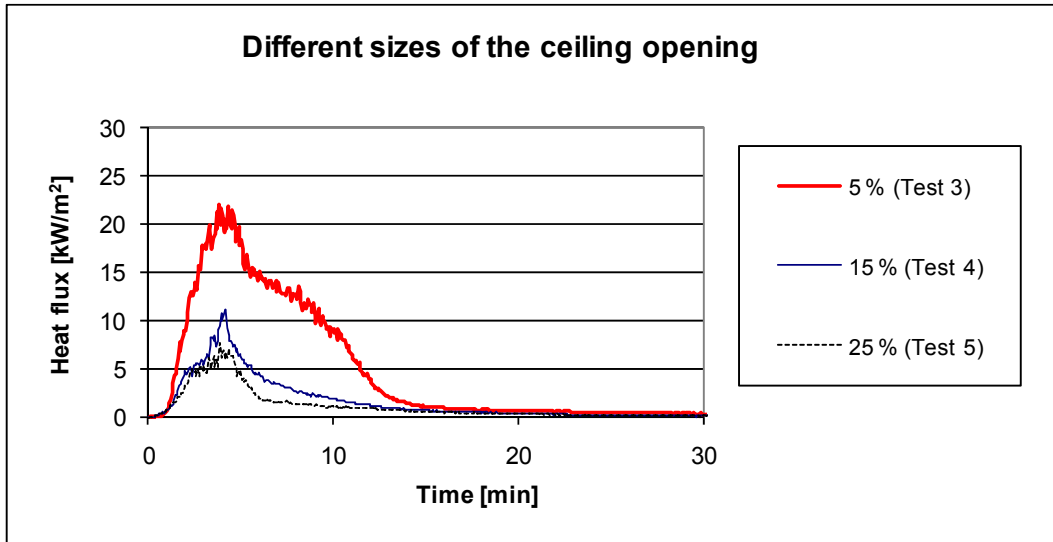


Figure 5.13 Heat flux curves, 1 m from the long wall, for tests with a) 5 % ceiling opening (Test 3), b) 15 % ceiling opening (Test 4), and c) 25 % ceiling opening (Test 5).

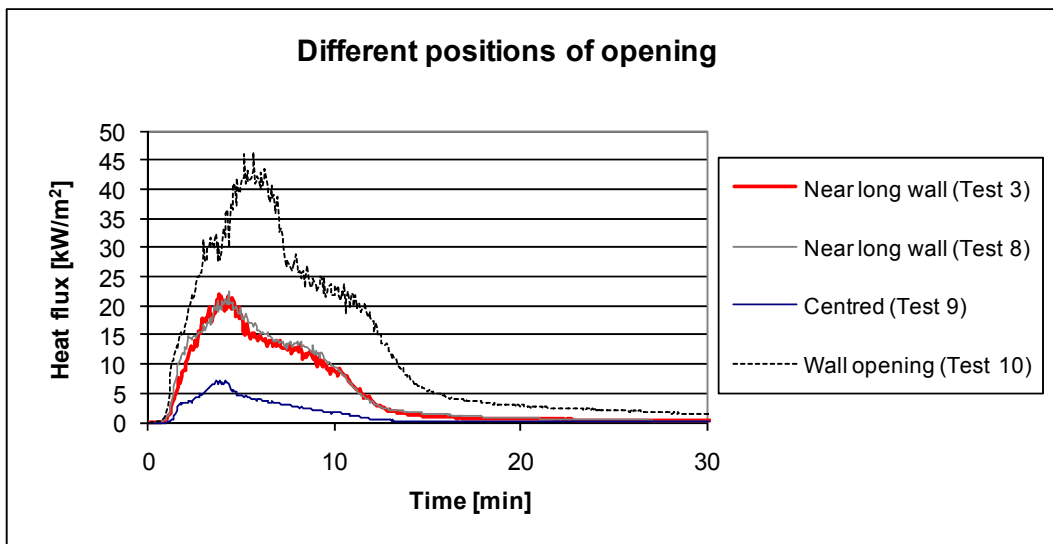


Figure 5.14 Heat flux curves, 1 m from the long wall, for tests with the same opening size (5 %), but different positions: a) in the ceiling near one of the long walls (Test 3), b) centred in the ceiling (Test 9), and c) as a wall opening (Test 10). Test 8 is included as a repetition test of Test 3.

In order to investigate the accuracy of the calculation methods presented in section 2.4, a comparison of the measured values was carried out for the heat flux meters. First, a comparison was carried out using equation (2), using the observed flame height. The distances were taken from the centre of the flame. For example a distance of 0.3 m was added for the 5 % opening, 0.9 m for the 15 % opening and 1.5 m for the 25 % opening, respectively, to the heat flux meter 0.5 m from the wall. The distance L in equation (2) is the distance from the heat flux meter to the centre of the flame volume, which means that the distance should be calculated as the diagonal distance from the heat flux meter up to half the flame length. Using Pythagoras rule, we can calculate the distance L . The HRR is known for each test, so the only parameter to calculate is L . In Figure 5.15, a plot based on calculated and measured data is shown. The fit is not good, there is a tendency that the calculation method strongly underestimates the heat fluxes, especially at positions relatively close to the flames.

It is known [43] that the radiance along a centreline of a flame is nearly constant up to about half the flame height (constant flame area), and decreases rapidly down to a value that is about 1-5 % of the maximum value at the flame tip. The same results may be observed when the excess gas temperature is measured along a vertical plume centreline [41]. Below about half the flame height (constant flame region), the excess gas temperature is approximately 800 °C ($E_f \sim 80 \text{ kW/m}^2$), but falls in the region of intermittent flaming to about 320 °C ($E_f \sim 7 \text{ kW/m}^2$) at the boundary of the buoyant plume. Based on this it can be argued that it is more appropriate to position the centre of radiance lower, in the range of $\frac{1}{4}$ - $\frac{1}{2}$ of the flame height. By changing the ratio we found that best agreement between measured and calculated was obtained when $\frac{1}{4}$ of the flame height was chosen. The results are shown in Figure 5.16. The agreement is much better here, and the data indicates that a use of $\frac{1}{4}$ of the flame height instead of $\frac{1}{2}$ the flame height when calculating the heat flux towards a certain measuring point, using Equation (2), is more appropriate.

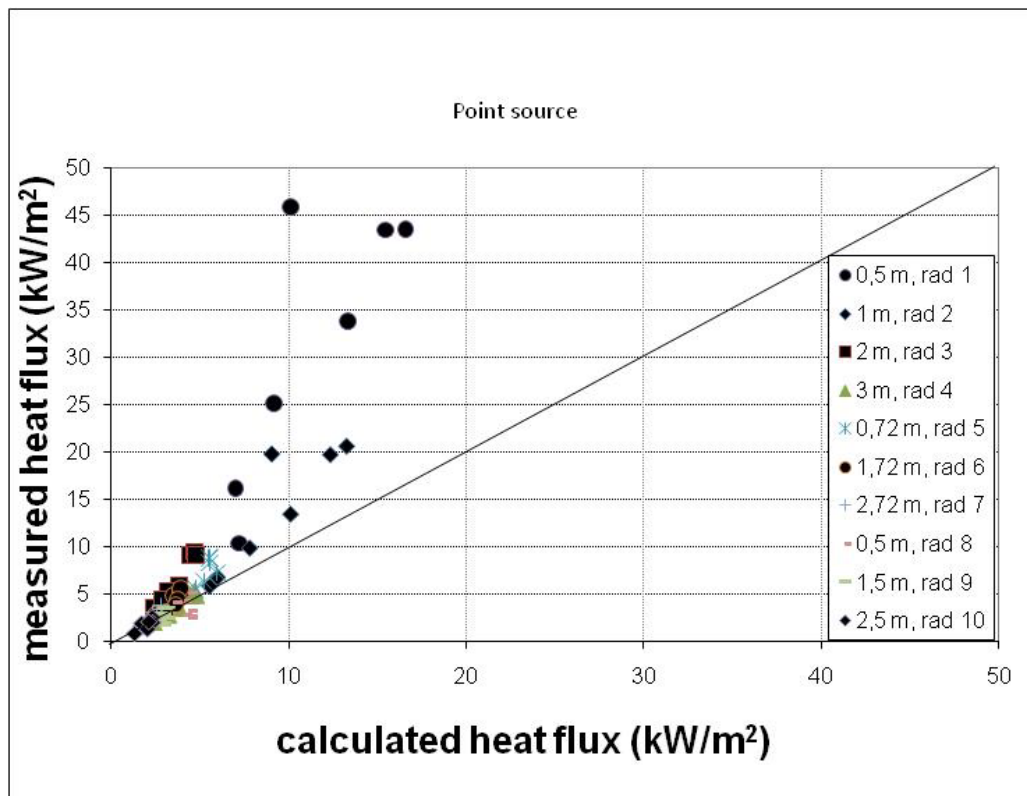


Figure 5.15 The maximum measured heat flux compared to the calculated heat flux (using Equation (2)) using $\frac{1}{2}$ the flame height for calculation of the distance.

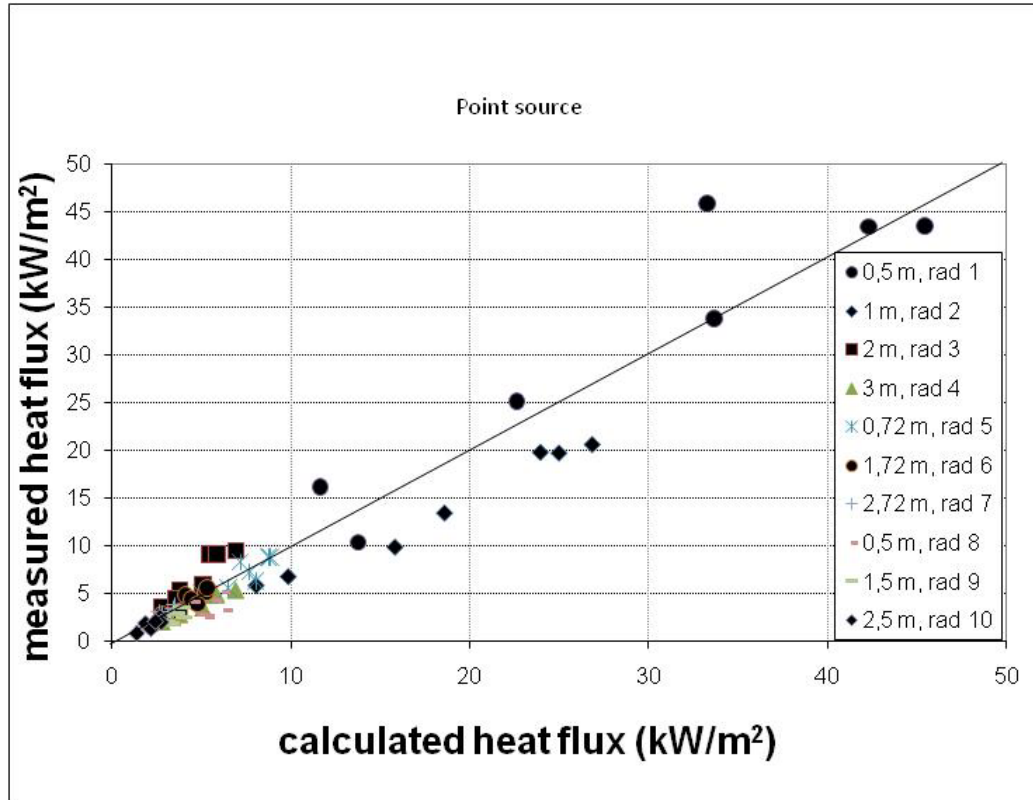


Figure 5.16 The maximum measured heat flux compared to the calculated heat flux (using Equation (2)) using $\frac{1}{4}$ the flame height for calculation of the distance.

A comparison was also done using the view factor method (solid flame model). In this case calculations and comparison were only performed for the heat flux meters positions that are perpendicular to the long wall of the building, i.e. the measuring points that are 0.5 m, 1 m, 2 m and 3 m, respectively, from the wall of the model building. The heat flux was calculated using equation (3) to (6), for these four points. The results are shown in Figure 5.17. Here we assume that $\tau=1$, $\epsilon=0,9$ and the view factor is calculated by equation (4) assuming the height is equal to the flame height. The gas temperature T_f is put equal to 800 °C. The results are very poor close to the wall, but become increasingly better as the distance increases.

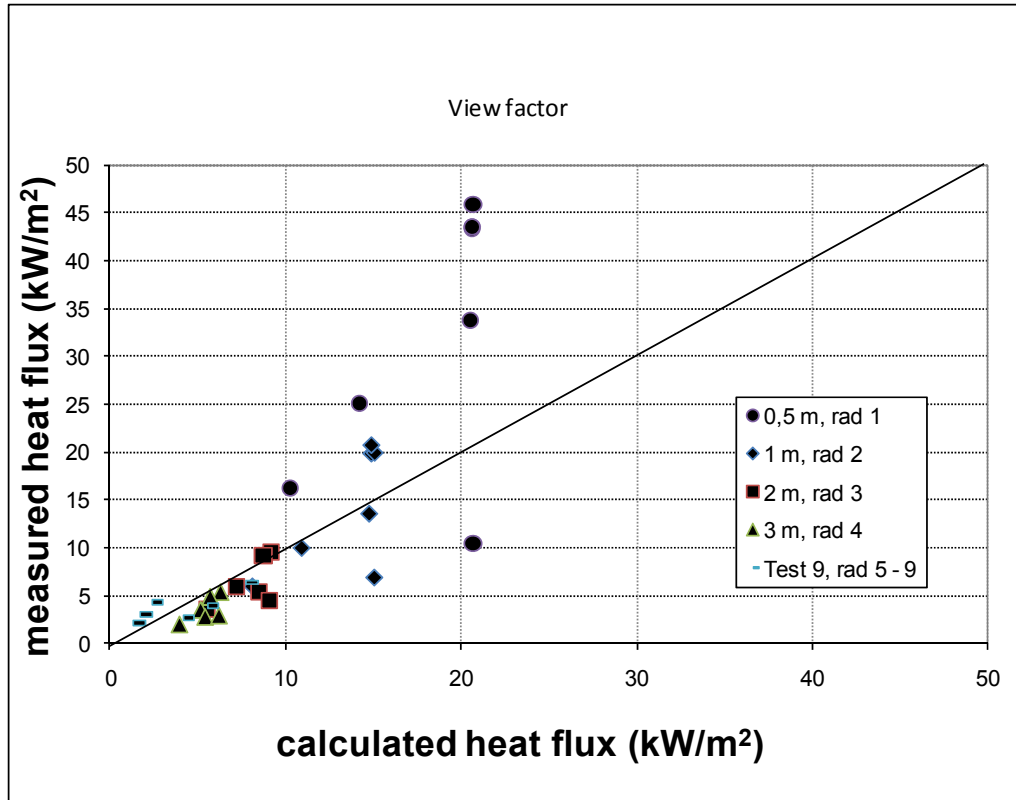


Figure 5.17 The maximum measured heat flux compared to calculated heat flux using the view factor method.

If we compare these two methods we can conclude that using $\frac{1}{4}$ of the flame height when calculating the diagonal distance to the flame in the point source model, yields the best results. There is a relatively poor correspondence using the view factor method, especially close to the fire source.

5.4.2 Comparison between plate thermometers and heat flux meters

There are several reasons for using plate thermometers instead of heat flux meters. The two main reason are that 1) the heat flux meters measure the heat flux to a cooled surface, which might not be a particularly good representation of reality, and 2) the plate thermometer is easier to use as it does not require any cooling water. Since heat flux meters have been used for a long time and are included in many standards it is, however, important to compare the behaviour of the two different types of measuring devices. In this section the results from such a comparison are presented. The graphs for each individual test are given in Appendix 2.

One can see from Figure 5.18 and Figure 5.19, which show Test 3 and Test 5, there is good correspondence between the measurements and the calculations. The heat flux for the Plate Thermometer (PT) was calculated using equation (10). There are, however, some minor differences that can be observed. There is an offset in the results from the heat flux meters, in particular for Test 1 and Test 2 (see Appendix 2) where the heat flux was very low. The reason for this is the calibration routine where the meters were calibrated for somewhat higher heat fluxes giving this offset for heat fluxes close to zero. A constant offset can also be seen in the values calculated from the PT. There is also a small difference in the maximum value.

In Figure 5.18 and Figure 5.19 the heat fluxes from the heat flux meters are compared to the results calculated from plate thermometers for distances of 0.5 m and 2 m, respectively. There is a good agreement between the two different types of measurement. That is also the case for other tests (see Appendix 2).

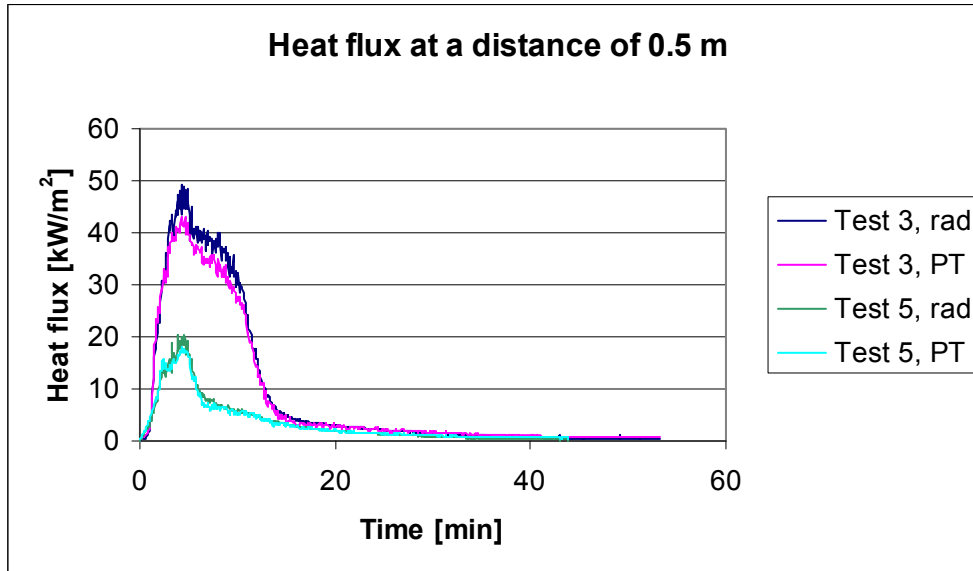


Figure 5.18 Comparison between results from heat flux meter and calculated heat flux from plate thermometers. The position is 0.5 m from the long wall of the scale model.

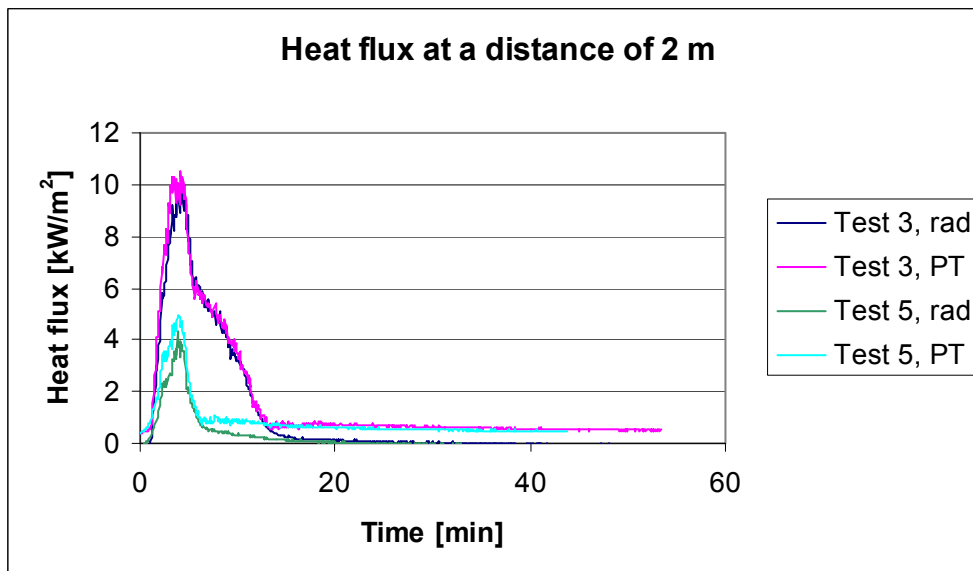


Figure 5.19 Comparison between results from heat flux meter and calculated heat flux from plate thermometers. The position is 2 m from the long wall of the scale model.

6 Discussion

A number of model-scale tests were conducted at a scale of 1:10. The main objective of the fire experiments was to study flame height and heat flux, and to evaluate the model used to estimate the risk of fire spread. The model had the dimensions of 6 m × 3 m × 0.7 m and simulated industrial premises in full scale measuring 60 m × 30 m × 7 m. The fire source used was large wood cribs, which was lit with the help of heptane. These fire sources were used to get as uniform a fire as possible for a relatively long period of time. The fire was expected to cover a large enough floor space to meet the widespread fires in industrial premises. A total of ten tests were performed. The number of openings and the opening area was varied to simulate ports of the building and holes in ceiling and walls. By collecting the combustion gases in a hood connected to the exhaust system, the HRR was measured (the most important design parameter). Together with the measured flame height and heat flux, different modelling techniques for incident radiation to neighbouring structures were validated.

The test results show that the opening size and placement in a significant way affect the radiation and the risk of fire spread. Compared to free burning conditions, the maximum HRR is increased by 14 % with 5 % opening in the ceiling and increased by 40 % for the case when the ceiling opening covered 15 % of the ceiling. It is interesting to note is that if the opening gets larger, some of the re-radiation effects are reduced and the HRR is also reduced. With the openings in the ceiling, the HRR become larger than when the opening is along the wall and it becomes larger if the opening is located centrally in the building than closer to the wall. This can be explained by the possibility of the fresh air coming in through the inlet openings to access to the combustion area. When the openings are centred in the ceiling the fresh air entrain more symmetric compared when the air can only access from one side. Further, when there are only small openings in the ceiling the fire becomes ventilation controlled. The highest HRR was only about one third of the free burn HRR.

The openings in the walls simulated open ports, and the results show that they have a significant influence on fire development. A simple port equivalent in full scale to 4 m × 4 m, and a double gate corresponding to 8 m × 4 m (in this case a double port on each gable was used with a total area representing 64 m² in full scale). The size of the hole in the ceiling was varied during the test series corresponding to 5 %, 15 % or 25 % of the total ceiling area.

The flame height from large building fires, where the ceiling of a building has collapsed, can be difficult to estimate, since it has been observed that when a fire becomes very large it is divided into a number of smaller fires. This leads to a situation where the maximum flame height is equal to or smaller than the width of the base of the fire. This has been discussed in the report, especially the limits for such phenomena $\frac{H_f}{D} < 0.5$. In the test series the flame height ratio $\frac{H_f}{D}$ varied between 0.5 - 10. This means that there was never a tendency for break-up of the flames.

It is also seen in the tests that the behaviour of the flames changed during the tests. In the beginning of the tests, during the intense phase, the flames fill the entire ceiling opening exiting with high intensity. During the later phase, on the other hand, the fire is more evenly distributed inside the room and the flames exiting the opening are less intense. The flames do not fill the entire opening during this period. The estimation of the flame height during the model-scale tests does have uncertainties, even if it is much less uncertain than the estimation of flame height of real fires in industrial premises.

Some theoretical aspects for the calculation of flame heights and heat fluxes are given. The flame height correlations are found to follow the traditional flame height correlations relatively well, but it is recommended to use a correlation that is based on the smallest width of the opening, equation (12). This is especially important if the opening is very long, but not that wide. The maximum flame heights varied from very low flames, when the openings in the ceiling were very small to the highest flames that were observed, about 3 m. This corresponds to a flame height of 30 m in full scale.

A comparison was made using the point source model for calculation heat fluxes at different distance from the flame. The traditional way of using the equation, i.e. assuming $\frac{1}{2}$ the flame height in order to calculate the distance between the fire source and the receiver (heat flux meter), did not work very well. By changing the position representing the radiation point source, it was found that the best agreement between measured and calculated heat fluxes was obtained when $\frac{1}{4}$ of the flame height was chosen instead. A comparison was also made using the view factor method (solid flame model). The results were found to be very poor close to the wall (fire), and become increasingly better as the distance increased.

To convert the lapse of time in the model scale test into full scale conditions, the measured times in model scale can be multiplied by approximately 3.2. It should, however, be noted that the focus of this study was the flames out through different openings and an evaluation of the risk for fire spread to other buildings, and not the fire development inside the original building.

The heat flux to the radiation meter that were positioned furthest away from the building was at a level that was 2-5 kW/m² and at the heat flux meter that were located closest, i.e. 0.5 m, up to 46 kW/m². The corresponding values in full scale, provided that the model is in 1:10 scale, is in the range of 6 to 15 kW/m² and up to 145 kW/m² at a distance which is 30 m and 5 m, respectively. This means that the validation of the models are covered within the range that is of interest in large scale i.e. 15 kW/m² and a distance that is up to 30 m.

There are some aspects that still need to be addressed, but have not been included in this study. Firstly, the effects of external wind on the flame height geometry is an issue that needs to be addressed. These effects are out of the scope of the present study. Secondly, in Sweden, a major concern has been raised about the new trend towards using sandwich constructions, which contains plastic foam material. In most cases, sandwich panels consist of plastic foam, mineral wool and steel sheet protection. The concern is focused on the consequences of a fire, i.e. combustible interior material may start to burn, and the fire can burn more easily through the ceiling and spread the fire inside the building due to dropping of plastic. This behaviour of the construction is important to the propensity of a fire to spread from one industrial facility to another but it was, unfortunately, not possible to include this in the present study as it is not possible to model such behaviour in a scale model.

7 Conclusion

The main conclusions from the study are:

- The test results show that size and position of openings significantly affects the radiation and the risk of fire spread.
- The openings in the short walls simulated open ports, and the results show that they have a significant influence on fire development.
- The flame height correlations were found to follow the traditional flame height correlations relatively well, but it is recommended that a correlation based on the smallest width of the opening, equation (12), is used
- The traditional way of using the point source equation for calculating incident heat flux, i.e. assuming $\frac{1}{2}$ the flame height in order to calculate the distance between the fire source and the receiver (heat flux meter), did not work very well. By changing the height ratio it was found that the best agreement between measured and calculated heat flux was obtained when $\frac{1}{4}$ of the flame height was chosen instead.
- A comparison was also made using the view factor method (solid flame model). The results were found to be very poor close to the wall (flame), and become increasingly better as the distance increased.
- The experimental variation covers the range of interest for validation of the models, i.e. corresponding to 15 kW/m^2 and a distance up to 30 m in real scale.
- The heat flux meters were compared to the results calculated from plate thermometers for distances of 0.5 m and 2 m, respectively. There is a good agreement between the two different types of measurement. This has practical implications for the way the heat flux can be measured or estimated using a significantly simpler method than traditional heat flux meters.

8 References

1. Boverket, *Regelsamling för byggande, BBR*, Boverket, Karlskrona, 2008.
2. NFPA, "Standard for Smoke and Heat Venting", NFPA 204, 2002.
3. Tuovinen, H., Ingason, H., and Lönnemark, A., "Industrial fires - A literature survey", SP Technical Research Institute of Sweden, SP Report 2010:17, Borås, Sweden, 2010.
4. Persson, H., "Evaluation of the RDD-measuring technique - RDD-tests of the CEA and FMRC standard plastic commodities", SP Swedish National Testing and Research Institute, SP Report 1991:04, Borås, Sweden, 1991.
5. Persson, H., "Commodity Classification: A more objective and applicable methodology", SP Swedish National Testing and Research Institute, SP REPORT 1993:70, Borås, Sweden, 1994.
6. Arvidson, M., and Lönnemark, A., "Commodity Classification Tests of Selected Ordinary Combustible Products", SP Swedish National Testing and Research Institute, SP REPORT 2002:03, Borås, Sweden, 2002.
7. Ingason, H., "Plume flow in high rack storages", *Fire Safety Journal*, **36**, p. 437 - 457, 2001.
8. Ingason, H., "Heat Release Rate of Rack Storage Fires", Proceedings of 9th Interflam - Fire Science & Engineering Conference, p. 731-740, Edinburgh, 17-19th September, 2001.
9. Ingason, H., "Effects of Flue Spaces on the Initial In-Rack Plume Flow", Fire Safety Science - Proceedings of the Seventh International Symposium, 235-246, Worcester, USA, 16-21 June, 2002.
10. Lönnemark, A., and Ingason, H., "Fire Spread in Large Industrial Premises and Warehouses", SP Swedish National Testing and Research Institute, SP Report 2005:21, Borås, Sweden, 2005.
11. Larsson, I., Ingason, H., and Arvidson, M., "Model Scale Fire Tests on a Vehicle Deck on Board a Ship", SP Swedish National Testing and Research Institute, SP Report 2002:05, Borås, Sweden, 2002.
12. Ingason, H., "Small Scale Test of a Road Tanker Fire", International Conference on Fires in Tunnels, pp. 238-248, Borås, Sweden, October 10-11, 1994.
13. Ingason, H., Wickström, U., and van Hees, P., "The Gothenburg Discoteque Fire Investigation", 9th International Fire Science & Engineering Conference (Interflam 2001), 965-976, Edinburgh, Scotland, 17-19 September, 2001.
14. Ingason, H., "Model Scale Tunnel Fire Tests - Longitudinal ventilation", SP Swedish National Testing and Research Institute, SP REPORT 2005:49, Borås, Sweden, 2005.
15. Ingason, H., "Model Scale Tunnel Fire Tests - Sprinkler", SP Technical Research Institute of Sweden, 2006:56, 2006.
16. Lönnemark, A., and Ingason, H., "The Effect of Cross-sectional Area and Air Velocity on the Conditions in a Tunnel during a Fire", SP Technical Research Institute of Sweden, SP Report 2007:05, Borås, Sweden, 2007.
17. Ingason, H., "Model scale tunnel tests with water spray", *Fire Safety Journal*, **43**, 7, pp 512-528, 2008.
18. Lönnemark, A., and Ingason, H., "The Influence of Tunnel Cross Section on Temperatures and Fire Development", 3rd International Symposium on Safety and Security in Tunnels (ISTSS 2008), 149-161, Stockholm, Sweden, 12-14 March, 2008.
19. Lönnemark, A., and Ingason, H., "The Effect of Air Velocity on Heat Release Rate and Fire Development during Fires in Tunnels", 9th International Symposium on Fire Safety Science, pp 701-712, Karlsruhe, Germany, 21-26 September 2008.

20. Ingason, H., and Lönnermark, A., "Effects of longitudinal ventilation on fire growth and maximum heat release rate", Proceedings from the Fourth International Symposium on Tunnel Safety and Security, pp 395-406, Frankfurt am Main, Germany, 17-19 March, 2010.
21. Heskestad, G., "Modeling of Enclosure Fires", Proceedings of the Fourteenth Symposium (International) on Combustion, 1021-1030, The Pennsylvania State University, USA, August, 1972.
22. Quintiere, J. G., "Scaling Applications in Fire Research", *Fire Safety Journal*, **15**, 3-29, 1989.
23. Saito, N., Yamada, T., Sekizawa, A., Yanai, E., Watanabe, Y., and Miyazaki, S., "Experimental Study on Fire Behavior in a Wind Tunnel with a Reduced Scale Model", Second International Conference on Safety in Road and Rail Tunnels, 303-310, Granada, Spain, 3-6 April, 1995.
24. Heskestad, G., "Physical Modeling of Fire", *Journal of Fire & Flammability*, **6**, p. 253 - 273, 1975.
25. Mudan, K. S., and Croce, P. A., "Fire Hazard Calculations for Large Open Hydrocarbon Fires". In *The SFPE Handbook of Fire Protection Engineering* (P. J. DiNenno, C. L. Beyler, R. L. P. Custer, W. D. Wilton, J. M. Watts, D. Drysdale, and J. R. Hall, Eds.), The National Fire Protection Association, 1995.
26. Tewardson, A., "Generation of Heat and Gaseous, Liquid, and Solid Products in Fires". In *The SFPE Handbook of Fire Protection Engineering* (P. J. DiNenno, D. Drysdale, C. L. Beyler, W. D. Walton, R. L. P. Custer, J. R. Hall, and J. M. Watts, Eds.), National Fire Protection Association, 3-109 -- 3-194, Quincy, MA, USA, 2008.
27. Siegel, R., and Howell, J. R., *Thermal Radiation Heat Transfer*, Third ed., Hemisphere Publishing Corporation, 1992.
28. Law, M., "Heat Radiation from Fires and Building Separation", Department of Scientific and Industrial Research and Fire Offices' Committee Joint Fire Research Organization, Fire Research Technical Paper No. 5, London, 1963.
29. Heskestad, G., "Fire Plumes, Flame Height, and Air Entrainment". In *The SFPE Handbook of Fire Protection Engineering* (P. J. DiNenno, Ed.), National Fire Protection Association, 2-1 -- 2-17, Quincy, Massachusetts, USA, 2002.
30. Heskestad, G., "Fire Plumes, Flame Height, and Air Entrainment". In *The SFPE Handbook of Fire Protection Engineering* (P. J. DiNenno, D. Drysdale, C. L. Beyler, W. D. Walton, R. L. P. Custer, J. R. Hall, and J. M. Watts, Eds.), National Fire Protection Association, 2-1 -- 2-20, Quincy, MA, USA, 2008.
31. Heskestad, G., "A reduced-scale mass fire experiment", *Combustion and Flame*, **83**, pp 293-301, 1991.
32. Wickström, U., "The Plate Thermometer - A simple Instrument for Reaching Harmonized Fire Resistance Tests", SP Swedish National Testing and Research Institute, SP REPORT 1989:03, Borås, Sweden, 1989.
33. Wickström, U., "Short Communication: Heat Transfer by Radiation and Convection in Fire Testing", *Fire and Materials*, **28**, 411-415, 2004.
34. Ingason, H., and Wickström, U., "Measuring incident radiant heat flux using the plate thermometer", *Fire Safety Journal*, **Vol. 42**, 2, 161-166, 2007.
35. Arvidson, M., and Ingason, H., "Measurement of the efficiency of a water spray system against diesel oil pool and spray fires", SP Swedish National Testing and Research Institute, SP Report 2005:33, 2005.
36. Häggkvist, A., "The Plate Thermometer as a Mean of Calculating Incident Heat Radiation - A practical and theoretical study", Luleå University of Technology, 2009.
37. Dahlberg, M., "The SP Industry Calorimeter: For rate of heat release measurements up to 10 MW", SP Swedish National Testing and Research Institute, SP REPORT 1992:43, Borås, Sweden, 1993.

38. Dahlberg, M., "Error Analysis for Heat Release Rate Measurement with the SP Industri Calorimeter", SP Swedish National Testing and Research Institute, SP REPORT 1994:29, Borås, 1994.
39. Huggett, C., "Estimation of Rate of Heat Release by Means of Oxygen Consumption Measurements", *Fire and Materials*, **4**, 2, 61-65, 1980.
40. Parker, W. J., "Calculations of the Heat Release Rate by Oxygen Consumption for Various Applications", National Bureau of Standards, NBSIR 81-2427, Gaithersburg, USA, 1982.
41. Drysdale, D., *An Introduction to Fire Dynamics*, John Wiley & Sons, 1994.
42. Lönnermark, A., and Ingason, H., "The Influence of Tunnel Dimensions on Fire Size", Proceedings of the 11th International Fire Science & Engineering Conference (Interflam 2007), 1327-1338, London, UK, 3-5 September, 2007.
43. Ingason, H., and DeRis, J., "Flame Heat Transfer in Storage Geometries", *Fire Safety Journal*, **31**, p. 39-60, 1998.

Appendix 1 Test protocols

In the test protocol notes, references are made to different openings. The openings O1 and O2 refer to the openings in the short walls. The openings V1 – V4 refer to the small ventilations openings in the ceiling (see Figure 3.2). When referring to the “ceiling opening” or the “wall opening”, reference is made to the openings simulating the burning through of the fire. The velocity measurements presented during the tests were made using a hand held velocity meter. When a flame height is given for the flames through the ceiling opening, the reference level is the ceiling and the height is measured from this level.

Test 1

-02:00	Measurement start
00:00	Ignition. All four pools ignited at the same time.
00:15	Moisture/smoke blocks half the height of window 4 Smoke out of the holes in the ceiling
00:21	Smoke filled the room
00:30	Smoke observed exiting the opening. Bi-directional flow observed in the inlet opening, 1/3 of height smoke out
00:53	Flames observed in ceiling, bended slightly, focused to the four pool fires, some notice that parts of wood crib had ignited
01:31	It appears as the fire became somewhat less intense: more smoke observed and less flames.
02:21	Velocity in inlet 0.55 m/s measured at ¼ of the total height. There is a bi-directional flow in the opening.
02:55	The flames “wanders” towards opening 1.
02:58	A pumping of air in inlet and outlet openings.
03:04	Flames out of hole 1 in the ceiling The alumina foil from the insulation has fallen down
03:42	Flames out through V1, 0.3 m – 0.4 m high. Only smoke through the other opening (V2 – V4).
05:49	The smoke from V3 and V4 is very powerful with high velocity; flames 0.3 m from V1.
07:10	The burning conditions appear stable. Flames out of V1.
07:55	A huge barrier of flames is observed at the edge of the wood crib. Flame height out through V1 and V2 is approximately 1 m
09:52	Powerful smoke columns rising from openings V# and V4. Flame height approximately 1 m through V1 and V2.
11:16	Bi-directional flow in O1. Inlet velocity approximately 0.3 m/s.
11:58	Pulsating flames, 1 m high, are observed.
12:00	The flames out through hole 1 and 2 are more than 1 m high. Smoke out through hole 3 and 4.
12:30	Flames out through O1.
13:08	Extinguishment with water since flames out of opening and burning in the wood in the opening.

Test 2

-02:00	Measurement start
00:00	Ignition. Pool 1, 2 and 4 ignited (numbering in the same order as the ventilation openings)
00:28	Smoke observed flowing out through O1.
00:38	Flames observed at the ceiling; radius of deflection approximately 0.5 m

01:10	Pool 3 was manually ignited
01:14	Very clear smoke layering in the entire room. About half the room height was filled with smoke. The flames were burning nicely inside.
01:52	About 0.3 m long flames were observed coming out of V1. Smoke was coming out of the other ventilation holes.
02:15	Flames 0.5-1.0 m from V1.
02:55	About 0.3 – 0.5 m long flames coming out of openings V1 and V2.
03:24	The flames can be observed all the way towards the inlet opening O1. Very close to flashover.
04:07	Flames observed from all outlet holes. The flame height about 0.3 to 0.5 m high.
04:28	The flame is coming out of O1.
04:33	Flames (0.5 m) observed from all ventilation holes. Small flames out through O2.
04:45	A flashover occurs.
05:01	About 0.7 m high flames coming out of ventilation opening V3 and V4. Flames also out through V1 and V2.
05:36	It is almost like a flow towards inlet opening O1, disturbing the outflow of hot gases. This may be the start of a imbalance of in and outflow at this inlet opening.
06:00	Four steady state vertical flames, about 1 m in height, coming out of opening 1-4. Here is the start of a steady state period.
06:17	Flames come out of inlet opening 2. The flames are some few decimetre above the ceiling height.
06:43	Sometime the flames out of holes V1-V4 disappeared. This was probably related to the temperature out of the holes. Also the flow conditions inside the compartment and the interchange of the flow due to the inlet openings may have influenced the results.
07:40	Steady flames of about 1 m high from opening V1-V4.
07:35	Large flames out through O2.
07:59	Steady flames out of O2, over 1 m high from upper edge of opening.
09:14	Similar conditions as earlier. It is observed that there are no flame at opening O1. It appears that the system has been stabilised with inlet flow at through opening O1 and outflow through ventilation openings V1-V4 and through opening O2.
11:17	Steady flames coming out of all openings, except opening O1.
11:20	Manual extinction in order to save the construction from too much exposure.

Test 3

-02:00	Measurement start
00:00	Ignition. Ignition of pool 1, 3 and 4.
00:04	Smoke out through the large ceiling opening.
00:28	Pool 2 manually ignited.
00:30	Half the compartment smoke filled, evenly distributed along the ceiling.
00:34	Smoke out through V4.
00:38	First flames out through large ceiling opening.
00:54	First flames out through V1.
01:05	Flames from heptane fire deflecting along the ceiling.
01:09	Flames, 1 m high, through the large ceiling opening.
01:13	First flames out through V4.
01:15	Some smoke out through O2.
01:26	Flames (20 – 30 cm high) observed through V1.
01:30	Flames, 2 – 2.5 m high, through the ceiling opening.

01:51	Large flames through large ceiling opening. Flame length about 3.5 m. The entire opening filled with flames.
02:20	The flame height is 3.5 m.
02:32	The entire wood crib is burning.
02:35	30 cm flames from V1 and 10 cm flames from V4.
03:16	Flames about 4 m high.
03:54	The entire wood crib is burning nicely. The intensity of the fire is high. 20 cm flames from V1, 15 cm flames from V4. The flame height from the large ceiling opening is 4 m.
04:00	Flames, approximately 20 cm, out through the ventilation opening.
05:43	The intensity is decreasing. Flame height about 3 m. 10 cm flames from V1, 10 cm flames from V4.
06:27	Small flames out through the ventilation opening.
07:00	The flame height is 3.5 m.
07:50	0.98 m/s in the centre of inlet opening O1.
08:34	Flame height 2 – 2.5 m.
09:15	Velocity 1.1 – 1.2 m/s in opening O2.
09:30	Flame height approximately 2 m.
09:45	The combustion within the compartment appears to be complete. No smoke.
10:30	The flame height is 2 m. No flames through V1 or V4.
11:00	The flames through the opening has decreased, to 1.5 m.
13:00	The flame height is 1 m.
14:30	Small flames inside the compartment.
17:30	Very small flames inside the compartment.
21:30	No flames, only glowing embers.

Test 4

-02:00	Measurement start.
00:00	Manual ignition.
00:07	All ignition sources ignited.
00:17	Flames from heptane source through ceiling opening.
01:00	A 20 cm thick smoke layer created inside the compartment.
01:15	Flame height approximately 1.5 m, sometimes 2 m.
01:18	Flames deflected under the ceiling adjacent to the opening. Some smoke from V1.
01:40	The flame height is 2.5 m.
02:00	The height of the vertical, uniform flames is 3.5 – 4 m.
02:10	Some smoke through V1 and V4
02:29	90 % of the wood crib is ignited. The flames are situated in the middle of the ceiling opening.
03:00	The flame height is 5 – 6 m.
03:25	Some smoke through V1.
04:00	The flame height is 5.5 – 6 m.
04:20	The gas velocity measured just inside the centre of O2 is 1.8 m/s.
05:10	The flame height is 3.5 m.
05:14	The gas velocity measured just inside O1 is 1.4 m/s.
05:45	The flame height is approximately 3.5 m. The intensity has been reduced considerably. Probably there is no heptane left.
06:11	The flame height is 2.5 m. The flames are in middle of opening.
07:17	The flame height is 1.5 – 2 m.
08:27	The flame height is 2 m.
09:00	The flame height is 2 m. There is a constantly burning fire in the wood crib, Nice flame in the middle of the opening.
09:46	The flame height is 1.5.

10:10 The gas velocity is 1.25 m/s in the centre of opening O2.
 10:15 The flame height is 1 m.
 10:45 The gas velocity is 1.3 m/s in the centre of opening O1.
 11:00 The flame height is 0.5 – 1 m.
 11:23 The flame height is 0.5 m.
 12:00 No flames out through the ceiling opening.
 13:54 Some smoke is exiting through the large ceiling opening.
 21:15 Only glowing embers.

Test 5

-02:00 Measurement start.
 00:00 Manual ignition.
 00:18 No direct spread within the wood crib.
 00:40 Four fires are burning inside the compartment.
 00:47 The flame height from the large ceiling opening is 1 m.
 01:00 It is still mainly four heptane fire. The flame height is 1 m above the ceiling.
 01:23 The fire has spread within the wood crib and has involved 50 %.
 01:30 The flame height is 2 m.
 01:40 It has now become one fire.
 02:00 No smoke in the compartment (no layer).
 02:10 The flame height is 3 – 3.5 m.
 02:11 75 % of wood crib ignited.
 02:30 The flame height is 3.5 – 4 m.
 03:14 95 % of wood crib ignited.
 03:41 Entire wood is crib burning. The flame height is 4 – 5 m. The flame is concentrated to centre of opening and did not fill the entire opening.
 04:40 The flame height is 4 m.
 04:50 The gas velocity measured just inside the centre of O2 is 1.65 m/s.
 05:09 The fire intensity is reduced. The heptan is probably consumed.
 05:30 The flame height is 1.5 – 2 m. Some sparks from the fire is following the plume.
 06:00 The gas velocity measured just inside the centre of O1 is 1.51 m/s.
 06:05 The flame height is 1.5 m.
 07:00 No smoke.
 The flame height is 1 – 1.5 m.
 07:45 The flame height is 1 m.
 08:30 The flame height is 1.5 m.
 08:40 The flame height is 1 m.
 09:00 About 1 m flame height; steady burning of wood crib.
 09:30 The flame height is 1 m.
 10:00 The flame height is 1 m.
 10:45 The flame height is 0.5 m.
 11:00 The flames reach approximately 0.5 m above the ceiling. Sometimes longer flames, 1 – 1.5 m exit the opening.
 11:30 The flame height is 0.5 m.
 The gas velocity is 0.5 – 0.6 m/s in the centre of opening O1.
 The gas velocity is 0.6 – 0.7 m/s in the centre of opening O2.
 12:00 Single small flames, approximately 20 cm, through the large ceiling opening.
 12:40 No flames out of the opening.
 15:30 It is only burning along the edges of the wood crib.

Test 6

-02:00 Measurement start.

00:00	Manual ignition.
00:10	All ignition sources ignited.
00:20	The flames impinge on ceiling.
00:30	Half the compartment is filled with smoke.
00:45	The four flames impinging on the ceiling touch each other in the centre.
01:00	The flame height is 1.5 m. A flame out through V4.
01:31	Flames out through openings V3 and V4 , some smoke some flame.
02:00	The flame height is 3 m.
02:30	The gas velocity in opening O1 is 1.27 m/s.
03:10	The flame height is 3 – 3.5 m. Smoke out through openings V3 and V4.
03:50	Flames out now and then through V4.
04:17	The gas velocity in opening O1 is 1.46 m/s.
04:28	The flame height is 3.5 m.
04:48	Air is sucked in through V1 and V2 and out through V3 and V4, black smoke in puffs.
05:33	The flame height is 3.5 m.
05:57	The flame height is 3 m. Black puffs of smoke through V3 and V4.
06:30	Quite an amount of smoke out through V3.
07:00	Flames out through V4. The gas velocity in opening O1 is 1.45 m/s.
08:00	The flame height is 2 – 2.5 m.
09:00	The flame height is approximately 2.5 m. No flames in the ventilation openings. The fire is starting to decrease.
09:15	Flames out through V3 and small flames out through V4.
10:00	The flame height is approximately 2 m, occasionally somewhat higher. Now and then flames out through V3 and V4.
12:25	The flame height is approximately 2 m.
13:00	The flame height is 1.5 – 2 m. Flames out through V3 and V4, 20 – 30 cm high flames. The gas velocity in opening O1 is 1.4 m/s.
13:37	The flame height is 1 – 1.5 m.
14:55	The flame height is 1 – 1.5 m. Flames out through V4.
17:00	The flame height is approximately 1 m. Small flames in the ventilation openings. It is burning in the seal of opening O2 (which is closed in this test).
18:00	The flame height is approximately 0.5 m. No flames in the ventilation openings.
18:30	Only occasional flames out through the ceiling opening.
19:30	No flames out through the ceiling opening.
20:00	Some flames inside the compartment.
24:00	Only glowing embers.

Test 7

-02:00	Measurement start.
00:00	Manual ignition.
00:08	All ignition sources ignited.
00:17	Flames impinging on the ceiling.
00:26	Half of the ceiling height filled with smoke.
00:30	First flame out through the ceiling opening.
01:06	Flames out through V4.
01:18	The flame is divided into two parts, 2 m high.
01:30	The flame height is 4 m. Small flames out through V1 and V4.
01:44	The flame height is 5 m. Flames through all ventilation openings.
02:24	The flame height is 5 m.
02:47	The entire wood crib is burning.
03:01	The flame height is more than 5 m. Flames through all ventilations openings.

03:30	The flame height is approximately 6 m.
03:50	The gas velocity in opening O2 is 0.46 m/s.
04:20	The gas velocity in opening O1 is 0.62 m/s.
04:41	The flame height is 4.5 – 5 m. The ceiling opening is filled with flames. Flames through all ventilation openings.
05:25	The flame height is 4 – 4.5 m.
06:07	The flame height is 3.5 – 4 m. A smoke layer is observed in the room.
07:12	The flame height is 4 m.
07:28	The flame intensity is decreasing. The entire wood crib is burning.
08:10	The flame height is 3 m.
09:24	The flame height is 3 m.
11:00	The flame height is 2.5 – 3 m.
11:45	The flame height is 2 m.
13:00	Very thin flames out through the ceiling opening.
14:20	No flames out through the ceiling opening.
15:00	Small flames in the compartment.
19:00	Only small flames at the outer edge of the wood crib.
21:20	Only glowing embers.

Test 8

-02:00	Measurement start.
00:00	Manual ignition.
00:05	All ignition sources ignited.
00:14	Flames impinging on the ceiling.
00:28	Flames starts to be deflected along the ceiling.
00:40	Constant flames out through the opening.
00:59	About 70 % of wood crib ignited.
01:10	The flame height is 1 m.
01:18	Flames out through V4, 20 cm.
01:38	Entire wood crib ignited.
01:50	The flame height is 3.5 m. Entire compartment filled with smoke.
02:05	Flames out through V1 (20 cm) and V4 (30 cm).
02:35	The gas velocity in opening O2 is 0.65 m/s.
02:50	The flame height is 4 m.
03:09	The gas velocity in opening O1 is 0.8 m/s.
04:12	Flames out through V1 and V4.
04:34	The flame height is 4 m.
04:50	Heavy smoke through all ventilation openings.
05:40	The flame height is 3 – 3.5 m. Small flames (20 cm) out through V1 and V4.
05:53	Entire ceiling opening filled with flames.
06:40	The wood crib is burning intensely.
07:00	The flame height is 2.5 – 3 m. Small flames out through V1 and V4.
07:20	The gas velocity in opening O1 is 0.51 m/s.
08:15	The gas velocity in opening O2 is 0.52 m/s.
08:45	The flame height is 2.5 m.
09:50	The flame height is 2 m. Small flames (10 cm) out through V4.
11:30	The flame height is 1 – 1.5 m.
12:05	The flame height is 0.5 m.
12:30	The flame height is 0.5 m.
13:00	Very little flames out through the opening.
14:00	No flames out through the opening.
18:00	Only glowing embers.

Test 9

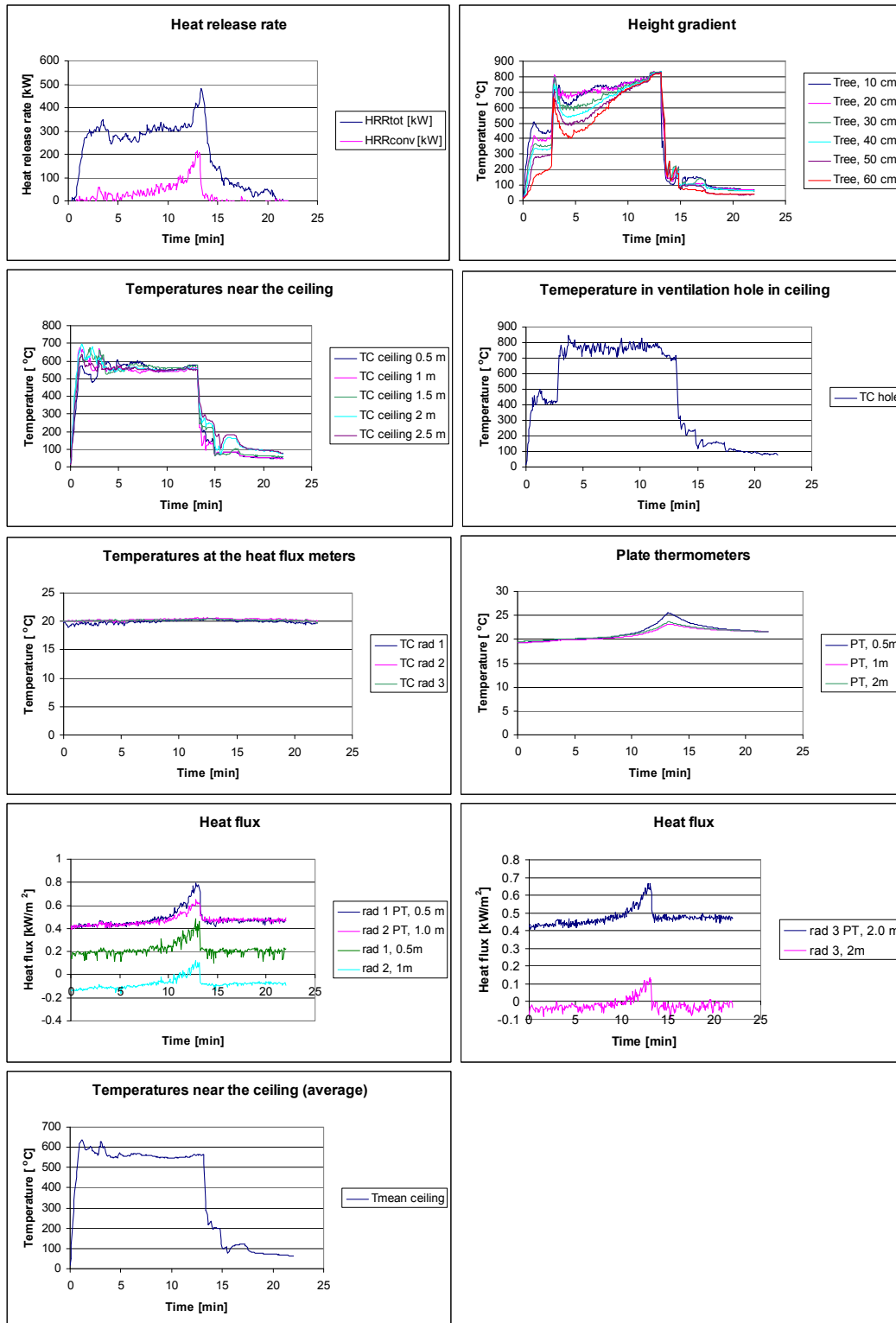
-02:00	Measurement start.
00:00	Manual ignition.
00:06	All ignition sources ignited.
00:18	Flames impinging on the ceiling.
00:52	Flames out through the opening.
01:00	The flame height is 0.5 m.
01:04	The fire spreads in the wood crib.
01:16	60 % of wood crib ignited.
01:24	80 % of wood crib ignited.
01:30	The flame height is 2 m.
01:36	90 % of wood crib ignited.
01:50	The flame height is 4 m.
02:00	95 % of wood crib ignited.
02:12	Entire wood crib burning.
02:20	The flame height is 4 – 4.5 m.
02:34	The flame height is 5 m.
03:00	The flame height is 5 m.
04:00	The flame height is 5 – 6 m.
	The gas velocity in opening O2 is 0.65 m/s.
04:35	The gas velocity in opening O1 is 0.67 m/s.
05:00	The flame height is 5 m.
05:14	The flame height is 4 m.
05:35	The flame height is 3.5 – 4 m.
06:15	The flame height is 3.5 – 4 m.
07:01	The flame height is 3 m.
07:46	The flame height is 2.5 m.
09:17	The flame height is 2 m.
10:45	The flame height is 1.5 – 2 m.
11:20	Smoke from all ventilation openings.
12:00	The flame height is 1 m.
13:00	The flame height is less than 0.5 m.
13:30	Occasional flames out through the ceiling opening.
13:45	No flames out through the ceiling opening.
19:00	Only small flames in the wood crib.
19:35	Only one small flame left.
21:04	The last flame is extinguished.

Test 10

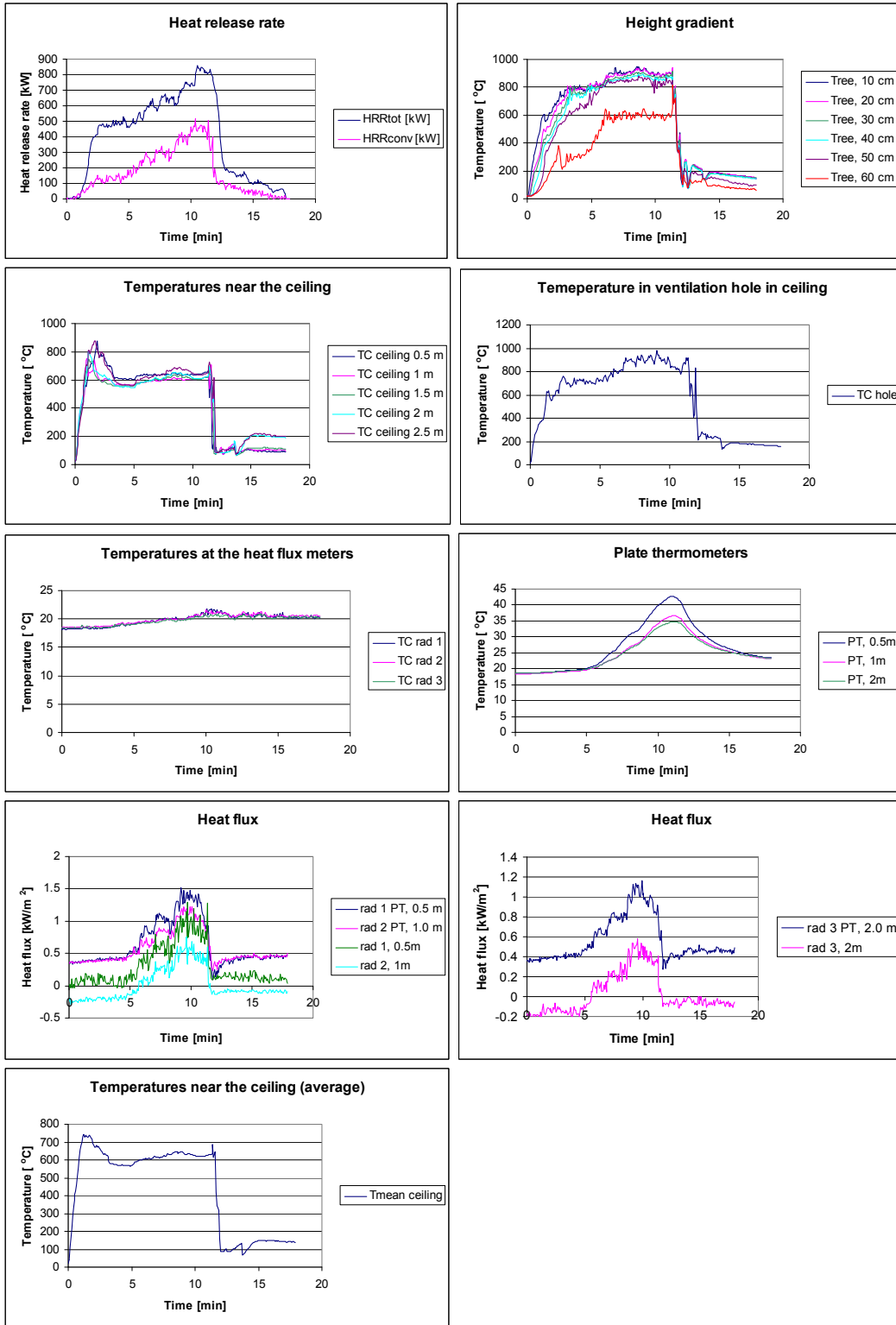
-02:00	Measurement start.
00:00	Manual ignition.
00:02	All ignition sources ignited.
00:50	Flames out through the opening.
02:00	The flame height is 1.5 – 2 m. Flames out through V1 and V4.
02:35	The flame height is 1.5 – 2 m.
08:00	The flame height is 1.5 m. Flames out through V1 and V4.
09:40	The flame height is 1 – 1.5 m.
11:40	Small flames out through V2.
13:20	The flame height is 0.5 – 1 m.
15:30	Almost no flames out through the wall opening.
16:30	No flames out through the wall opening.
20:00	Only small flames in the wood crib.
20:35	Only glowing embers.

Appendix 2 Time-resolved graphs

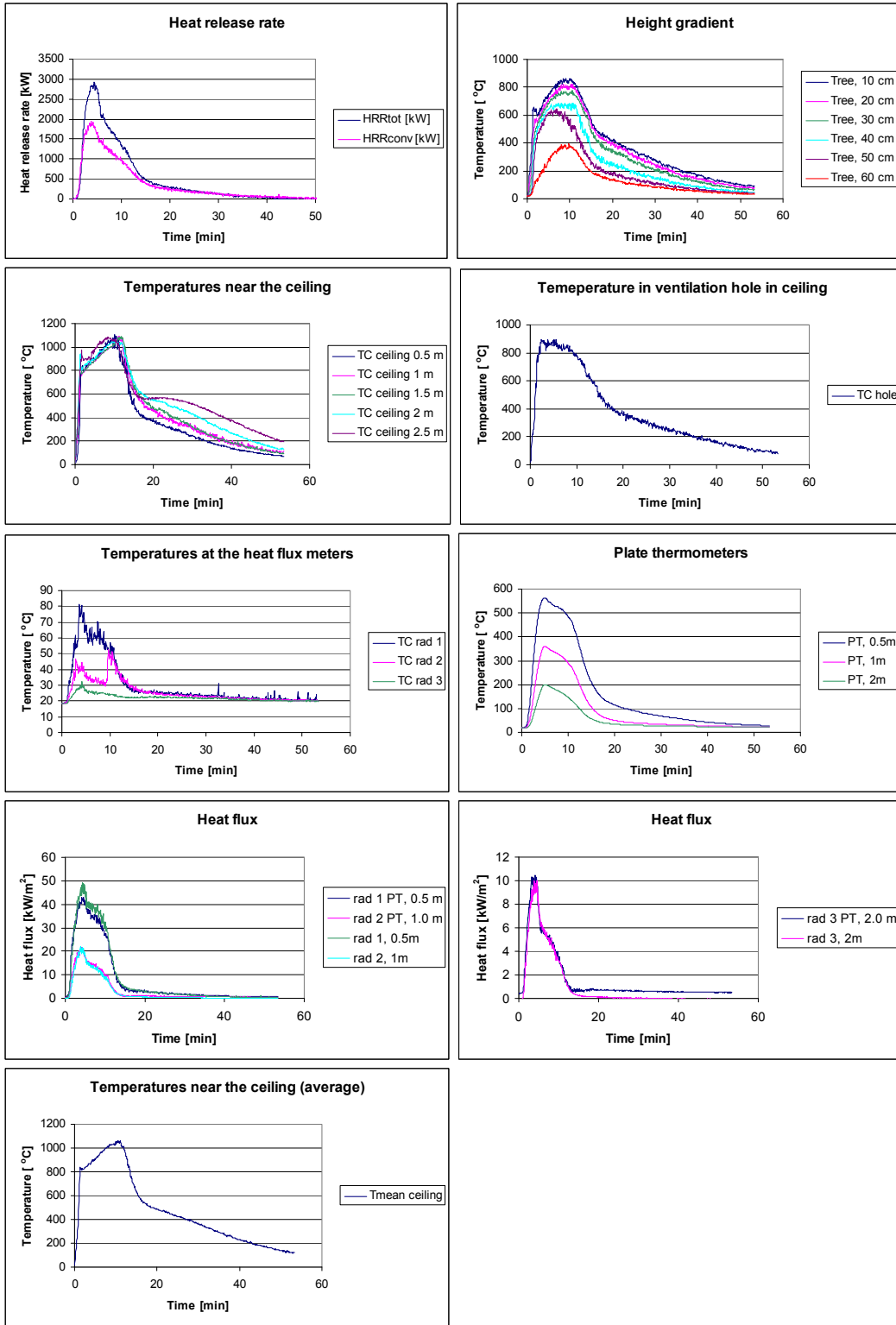
Test 1



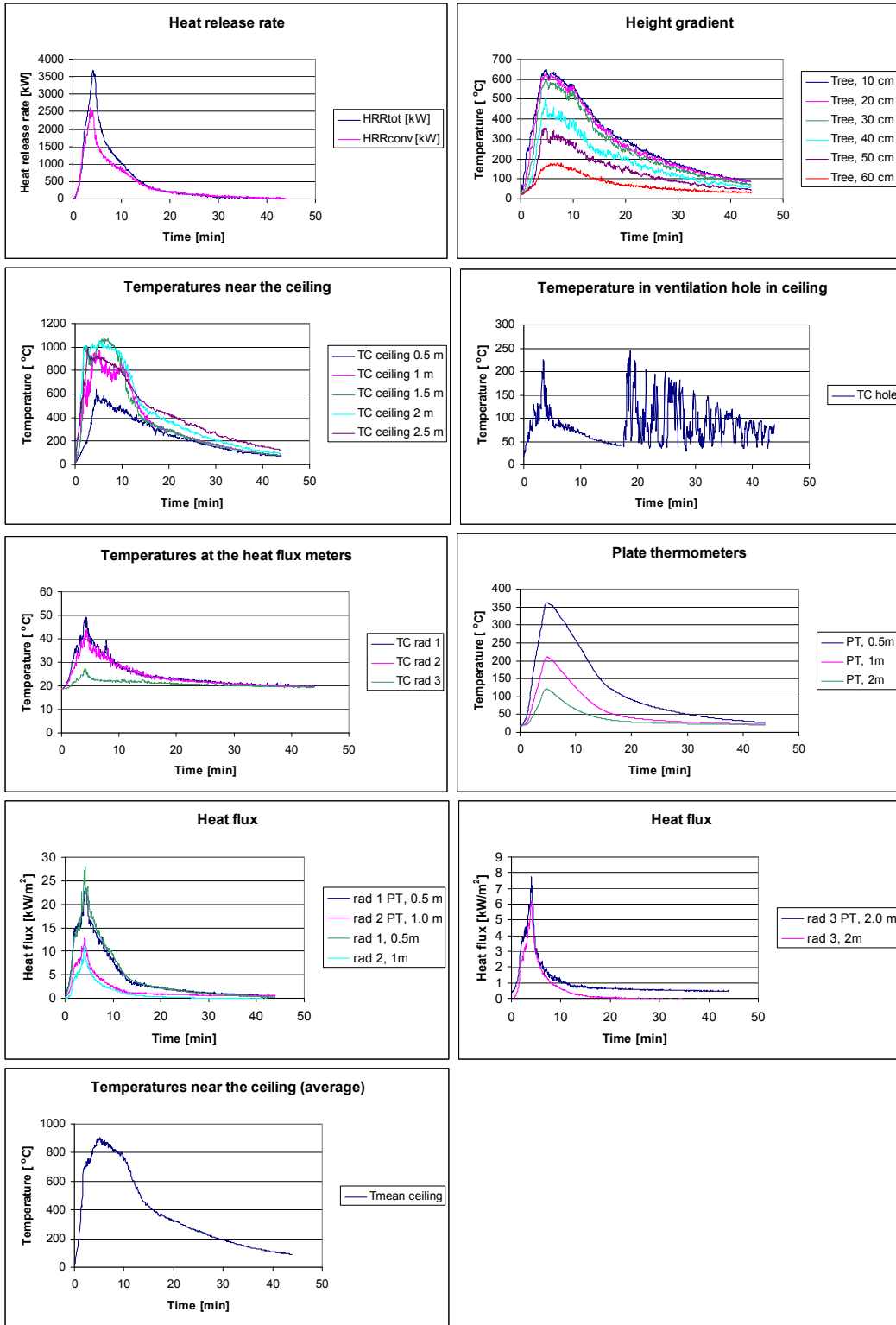
Test 2



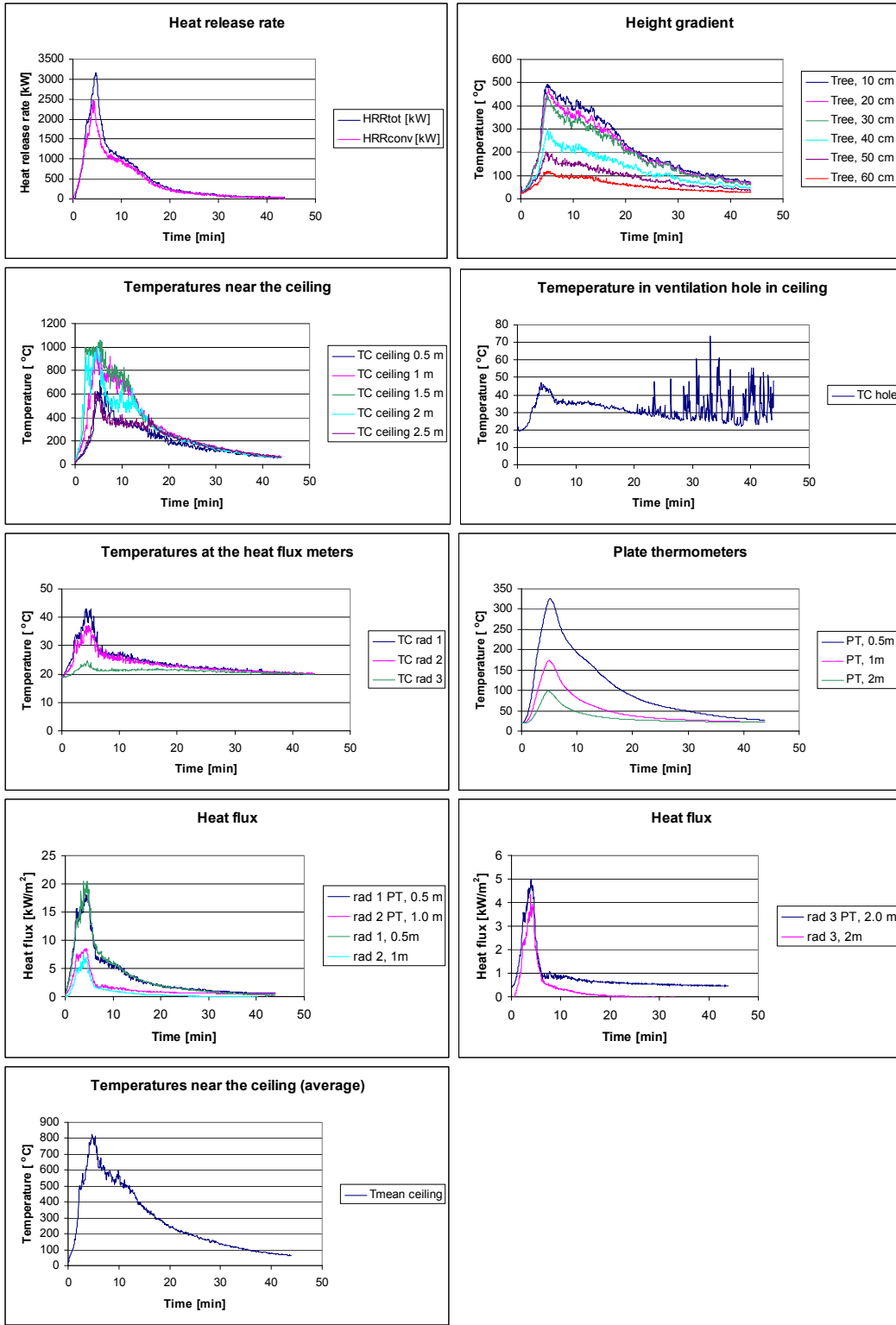
Test 3



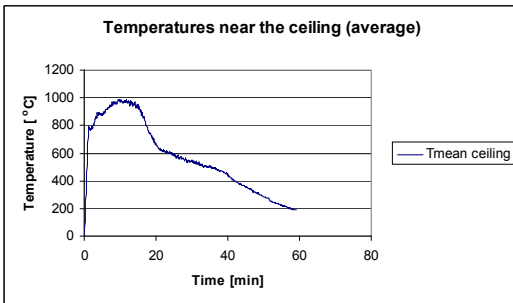
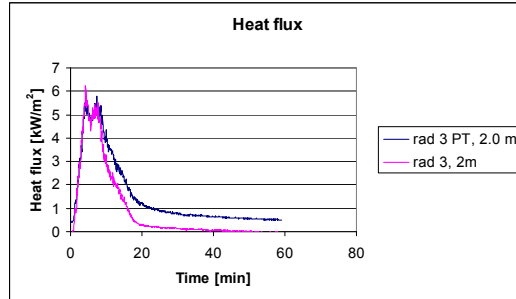
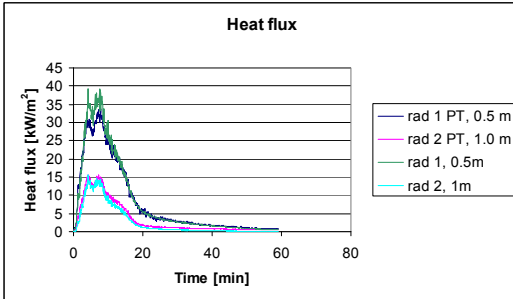
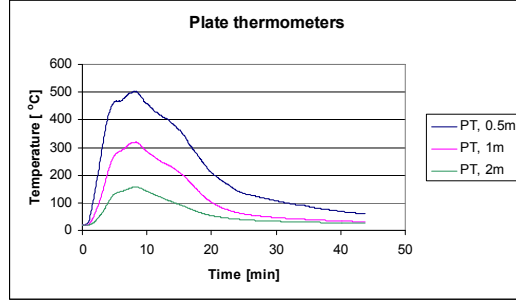
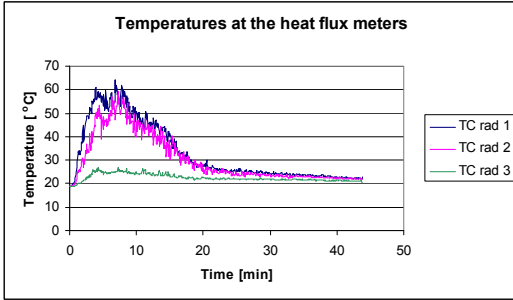
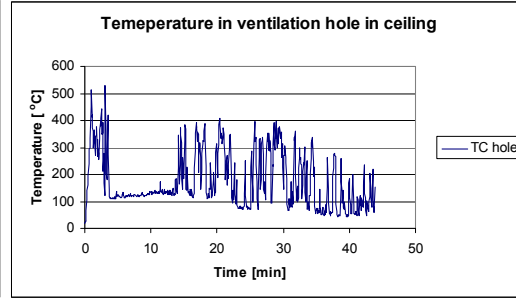
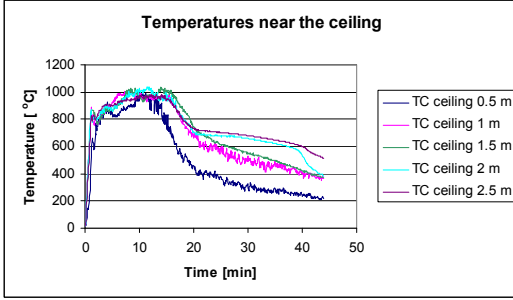
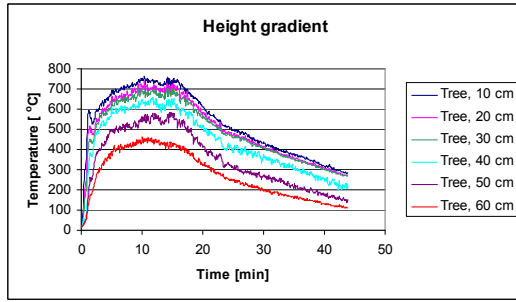
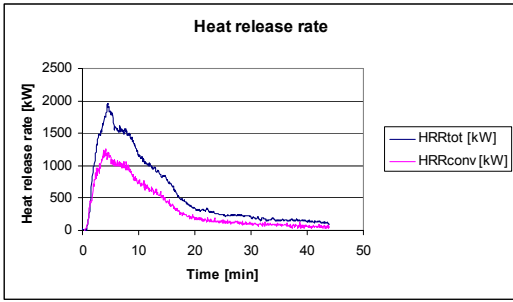
Test 4



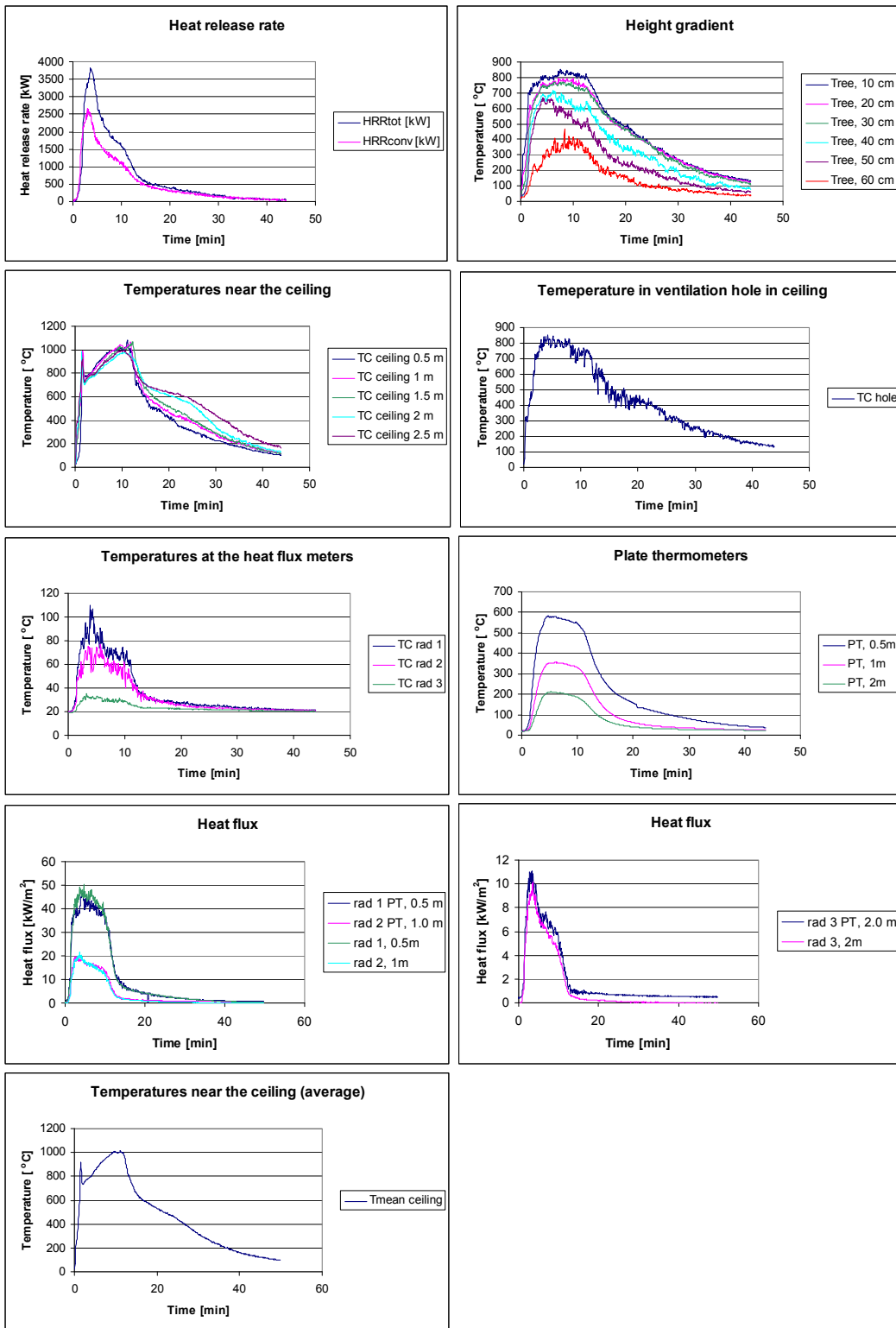
Test 5



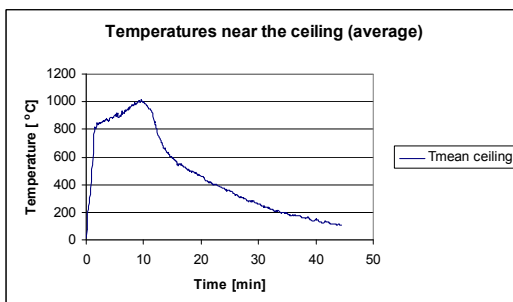
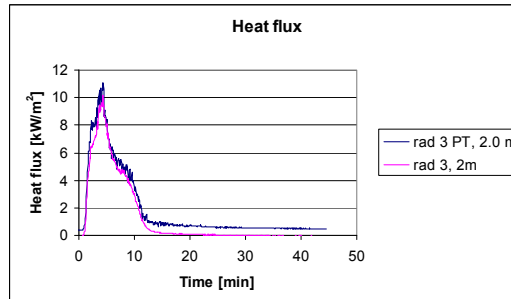
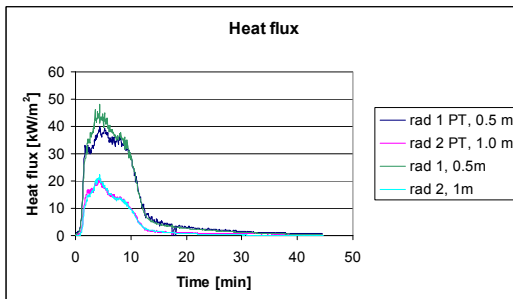
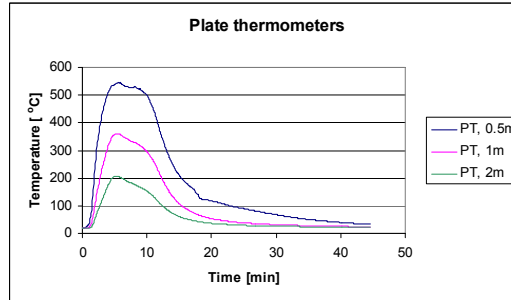
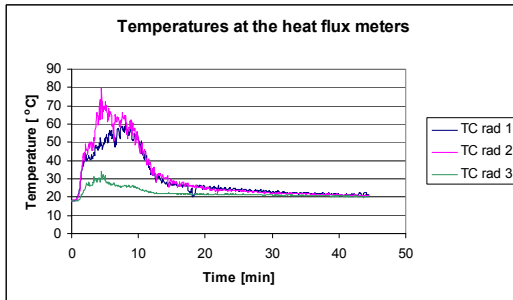
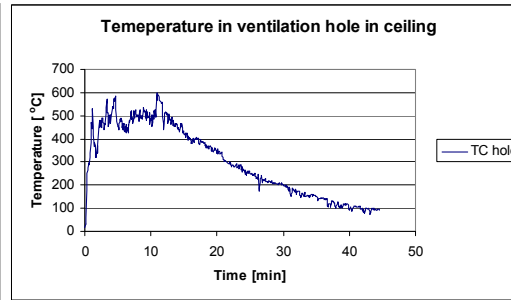
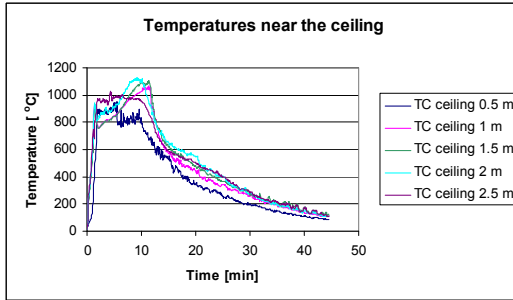
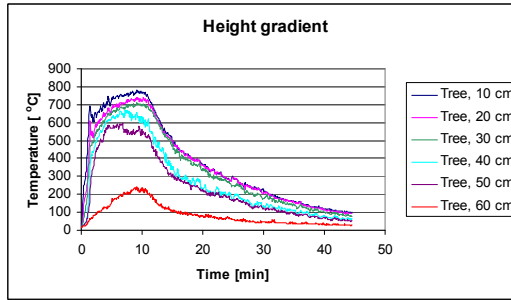
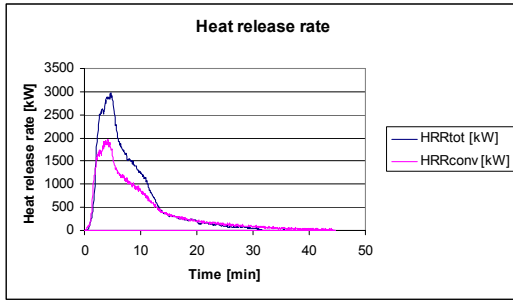
Test 6



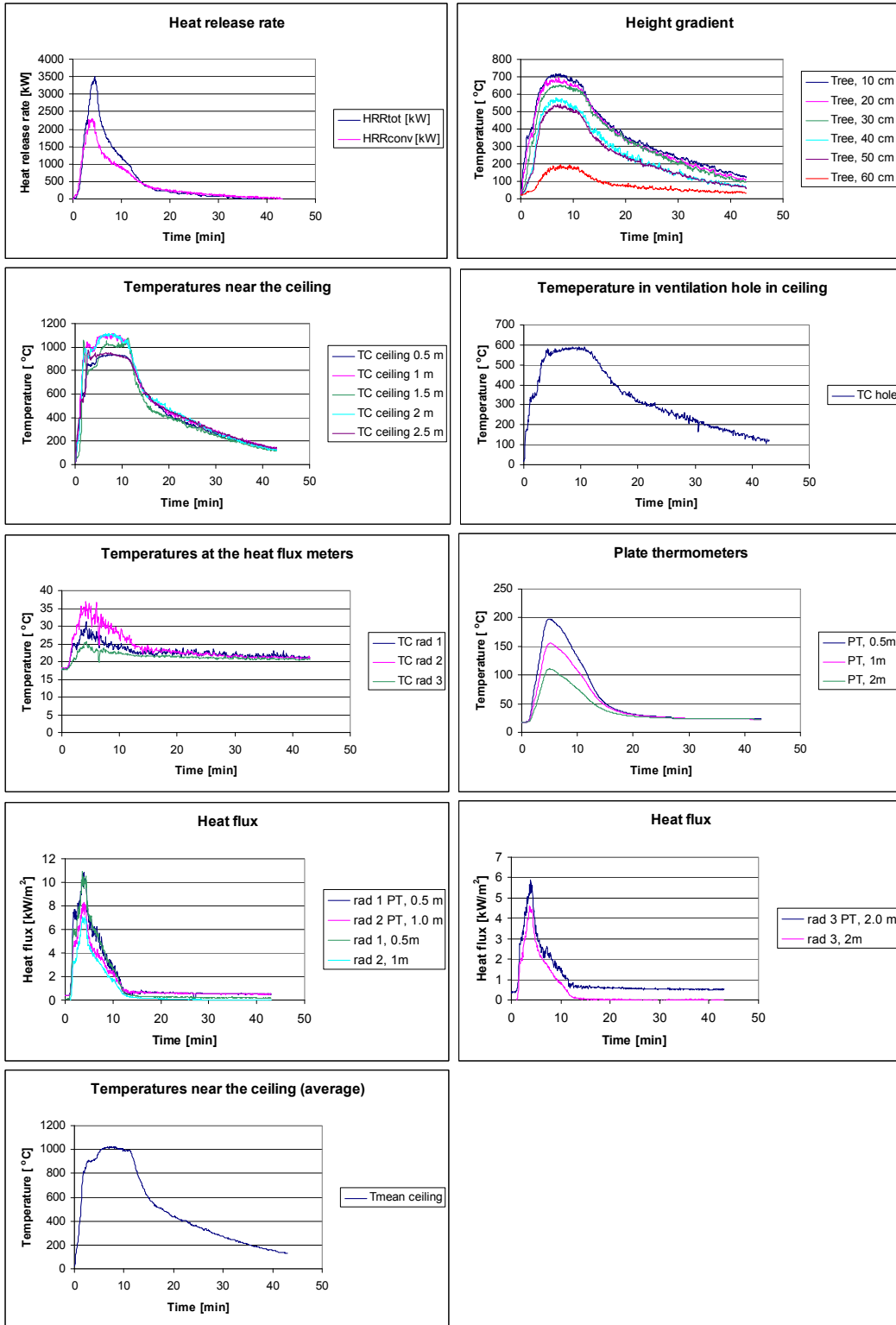
Test 7



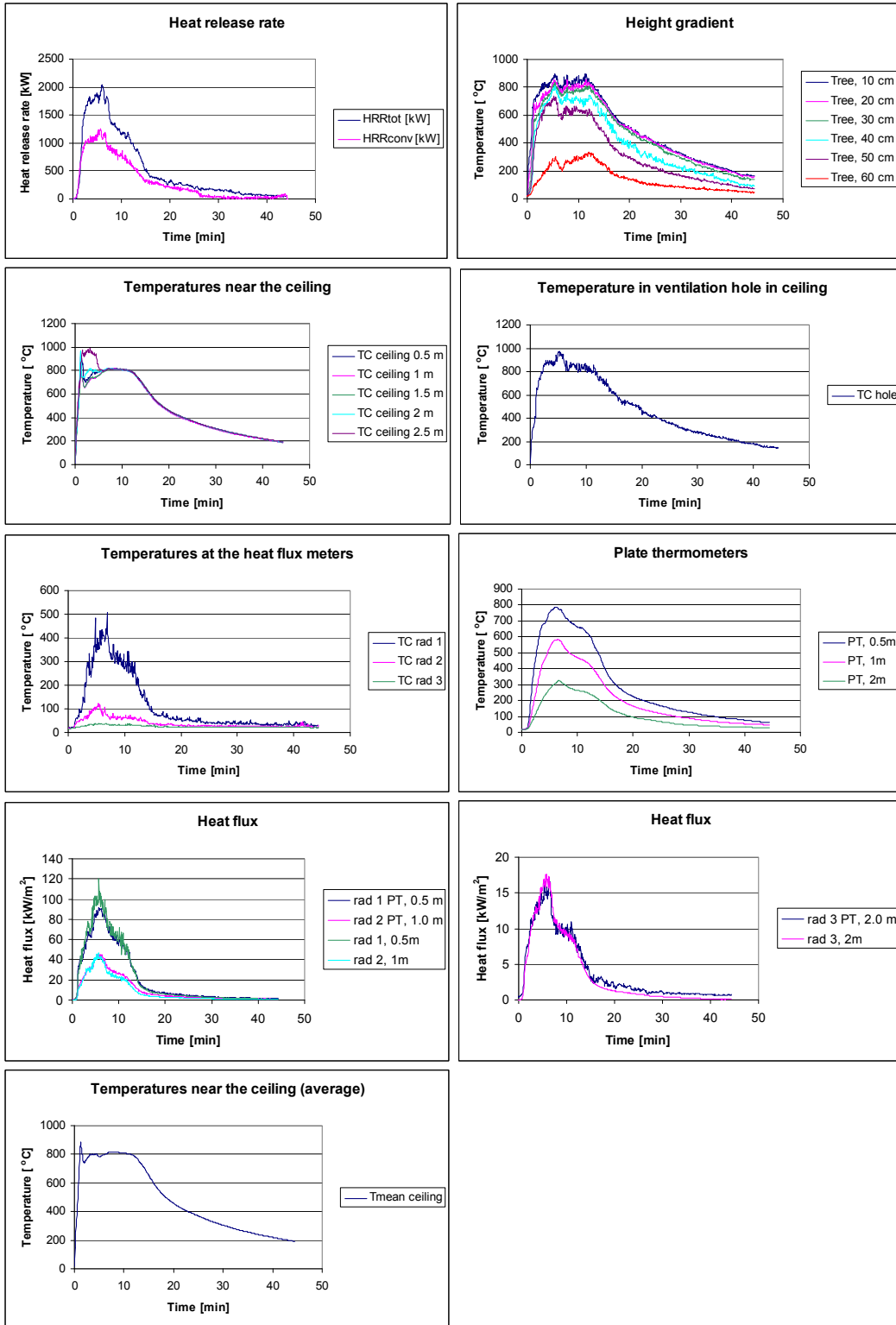
Test 8



Test 9

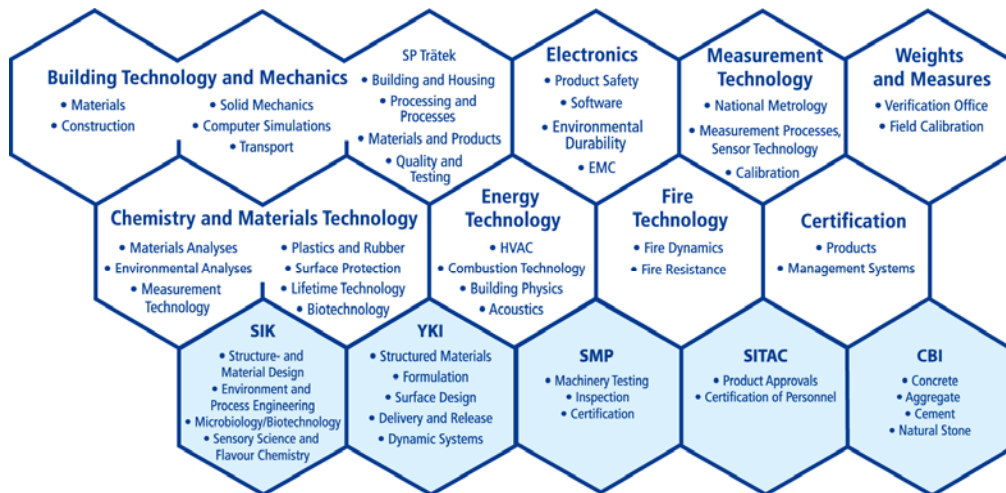


Test 10



SP Technical Research Institute of Sweden develops and transfers technology for improving competitiveness and quality in industry, and for safety, conservation of resources and good environment in society as a whole. With Sweden's widest and most sophisticated range of equipment and expertise for technical investigation, measurement, testing and certification, we perform research and development in close liaison with universities, institutes of technology and international partners.

SP is a EU-notified body and accredited test laboratory. Our headquarters are in Borås, in the west part of Sweden.



SP is organised into eight technology units and five subsidiaries



SP Technical Research Institute of Sweden

Box 857, SE-501 15 BORÅS, SWEDEN

Telephone: +46 10 516 50 00, Telefax: +46 33 13 55 02

E-mail: info@sp.se, Internet: www.sp.se

www.sp.se

Fire Technology

SP Report 2010:18

ISBN 978-91-86319-56-4

ISSN 0284-5172